Event and seasonal hydrologic connectivity patterns in an agricultural headwater catchment

Lovrenc Pavlin[1,2], Borbála Széles[1,2], Peter Strauss[3], Alfred Paul Blaschke[1,4], Günter Blöschl[1,2]

[1]Centre for Water Resource Systems, Vienna University of Technology, Vienna, Austria
[2]Institute of Hydraulic Engineering and Water Resources Management, Vienna University of Technology, Vienna, Austria
[3]Federal Agency of Water Management, Institute for Land and Water Management Research, Petzenkirchen, Austria
[4]Interuniversity Cooperation Centre Water & Health, Vienna, Austria

Correspondence to: Lovrenc Pavlin (pavlin@hydro.tuwien.ac.at)

Abstract. Connectivity of the hillslope and the stream is a non-stationary and non-linear phenomenon dependent on many controls. The objective of this study is to identify these controls by examining the spatial and temporal patterns of the similarity between shallow groundwater and soil moisture dynamics and streamflow dynamics in the Hydrological Open Air Laboratory (HOAL), a small (66 ha) agricultural headwater catchment in Lower Austria. We investigate the responses to 53 precipitation events and the seasonal dynamics of streamflow, groundwater and soil moisture over two years. The similarity, in terms of Spearman correlation coefficient, hysteresis index and peak-to-peak time, of groundwater to streamflow shows a clear spatial organisation, which is best correlated to topographic position index, topographic wetness index and depth to the groundwater table. The similarity is greatest in the riparian zone and diminishes further away from the stream where the groundwater table is deeper. Soil moisture dynamics show high similarity to streamflow but no clear spatial pattern. This is reflected in a low correlation of the similarity to site-characteristics, however, the similarity increases with increasing catchment wetness and rainfall duration. Groundwater connectivity to the stream on the seasonal scale is higher than that on the event scale indicating that groundwater contributes more to the baseflow than to event runoff.

1 Introduction

Hydrologic~~Hydraulic~~ connectivity is an important control on runoff generation in response to precipitation events (van Meerveld et al., 2015; Penna et al., 2015; Zuecco et al., 2016). It is usually defined as the ability of water, solutes or microorganisms to move from one landscape unit to another along a water flow path (Blume and van Meerveld, 2015; Saffarpour et al., 2016; Vidon and Hill, 2004). In the headwater catchments, the connection between the hillslope and the stream is established either when the groundwater table rises above the confining layer at the upland-riparian zone interface to a more permeable layer or when a permeable layer gets continuously saturated (Ocampo et al., 2006; Tromp-van Meerveld and McDonnell, 2006; Vidon and Hill, 2004). Changes in connectivity could be related to the differences in the patterns in hydrologic behaviour by considering the underlying controlling processes (Western et al., 2001). Therefore, the analysis of groundwater dynamics in different landscape units and across temporal scales is an important step toward understanding when and where the connectivity occurs.

Groundwater (GW) and soil moisture (SM) dynamics exhibit spatial patterns that can depend on site-characteristics such as soil depth (Penna et al., 2015; Rosenbaum et al., 2012), soil type (Gannon et al., 2014), land cover (Bachmair et al., 2012; Emanuel et al., 2014) and topography (Bachmair and Weiler, 2012; Rosenbaum et al., 2012). Surface and subsurface topography were shown to be important controls on the spatial distribution of groundwater dynamics and connectivity of the hillslope to the riparian zone and the stream (Bachmair and Weiler, 2012; Detty and McGuire, 2010; Loritz et al., 2019; Tromp-van Meerveld and McDonnell, 2006). Local slope affects the rainfall drainage, and the upslope contributing area affects the amount of water that could potentially be supplied to a given location as quantified by the Topographic wetness index (TWI)(Beven and Kirkby, 1979). The TWI was shown to be a good predictor of hydrologic connectivity ~~I~~in steep forested and grassland catchments with shallow groundwater table~~, upslope contributing area and TWI were shown to be good predictors of hydrologic connectivity~~ (Emanuel et al., 2014; Loritz et al., 2019; Rinderer et al., 2016, 2017) and

abandoned terraces (Lana-Renault et al., 2014; Latron and Gallart, 2008), while in some studies this ~~relationship existed~~was true only during specific wetness conditions, ~~or~~ for certain types of rainstorms (Bachmair and Weiler, 2012) or when terrain freezes over (Coles and McDonnell, 2018).

Antecedent wetness conditions and precipitation event characteristics, such as rainfall intensity and depth and antecedent wetness conditions have been also identified as important controls on groundwater and soil moisture responses to rainfall events (Dhakal and Sullivan, 2014; Penna et al., 2015; Rosenbaum et al., 2012; Saffarpour et al., 2016). Penna et al. (2015) and Detty and McGuire (2010) found that wetter antecedent conditions and higher rainfall depth increased groundwater peaks, the number of activated wells and the spatial extent of the subsurface flow network in a steep catchment in the Italian Alps and a forested catchment in New Hampshire, respectively. ~~In two steep Alpine catchments in Italy (Penna et al., 2015) and forested catchments in New Hampshire (Detty and McGuire, 2010) studies found that wetter antecedent conditions and higher rainfall depth increased groundwater peaks, the number of activated wells and the spatial extent of the subsurface flow network.~~ In contrast, groundwater in the Black Forest in Germany responded more weakly and slowly during wet conditions than during dry conditions when preferential flowpaths were activated (Bachmair et al., 2012). Rosenbaum et al. (2012) found that the rainfall characteristics, especially rainfall intensity, were the dominant controls on the soil moisture responses during the wetting period in a hilly forested test site Wüstenbach, Germany.

Seasonal and event dynamics of streamflow, groundwater and soil moisture may be governed by different processes in the catchment. Slower processes or flowpaths with lower celerity are normally more relevant on the seasonal scale, while the quicker processes control the event responses and do not affect the seasonal dynamics. Event dynamics is superimposed on the seasonal dynamics, which provides the initial conditions for the event flowpaths activation. Which site- or event-characteristics govern these changes in flowpaths is not explicitly clear. For example, Grayson et al. (1997) found that soil moisture in the humid temperate region of Australia transit between two preferred states: wet and dry. The wet state is controlled by lateral water movement related to catchment terrain, while the dry state is dominated by vertical water movement controlled by the local terrain and soil characteristics. Separation of temporal scales could also be linked to a separation of scales in space (Széles et al., 2018). To uncover these changes in flowpaths it is necessary to systematically investigate both short-term (event) and long-term (seasonal) dynamics on the catchment-wide scale. Differences in the similarity of the event and seasonal streamflow, groundwater and soil moisture dynamics could potentially indicate dominant controls on the flowpath activation and conversely connectivity of different landscape units.

Despite significant improvement in our understanding of the hillslope connectivity to the stream, the controls of the site- and event-characteristics on the groundwater and soil moisture dynamics in relation to the streamflow on the event and seasonal scale are not fully understood. Furthermore, in agricultural catchments, the hydrologic connectivity is also important for its impact on the solutes load (e.g. nitrate and dissolved organic carbon) in streams (Aubert et al., 2013; Zhang et al., 2011). Understanding of catchment connectivity could therefore lead to better agricultural practices, but except for Saffarpour et al. (2016) and Ocampo et al. (2006), the focus of the recent connectivity studies was less on the agricultural ~~landscape~~ catchments compared to forested and alpine catchments. Here we present an investigation of connectivity between the groundwater, soil moisture and streamflow in term of the similarity of their dynamics and how it is related to the site and event-characteristics. We analysed the similarity between individual groundwater and soil moisture monitoring stations and to the streamflow at the catchment outlet for 53 events and over two years to address the following questions:

1. What are the spatial and temporal patterns in the relationship between the streamflow, groundwater and soil moisture responses to precipitation events in an agricultural headwater catchment?
2. Is the relationship between the streamflow and groundwater or soil moisture dynamics more related to site- or event-characteristics?
3. How are event and seasonal connectivity of groundwater and soil moisture to streamflow related?

2 Methods

2.1 Study site

The research area of this study is the HOAL (Hydrological Open Air Laboratory) in Petzenkirchen, Lower Austria, about 100 km west of Vienna (Fig. 1) (Blöschl et al., 2016a). This is a headwater catchment with a catchment area at the outlet (termed MW) of 66 ha. The 620 m long Seitengraben stream is perennial with mean streamflow of 3.1 and 2.4 l/s in 2017 and 2018, respectively. The land use of the catchment is predominantly agricultural as 87% of the area is arable land, 5% are meadows, 6% is forested and 2% is paved. The most common crops are maize, winter wheat and rapeseed. The topography is hilly with an elevation range from 268 to 323 m a. s. l. and a mean slope of 8%.

The climate is humid with mean annual (2002-2018) precipitation of 781 mm/year, air temperature of 9.3 °C, runoff of 170 mm/year and evapotranspiration of 612 mm/year (assuming negligible deep percolation). Investigated years of 2017 and 2018 were dry compared to the long-term (2002-2018) average with 736 mm and 656 mm of rainfall, respectively. While monthly precipitation peaks in the summer, monthly runoff tends to peak in winter or early spring when the soil moisture and groundwater levels are highest (Széles et al., 2018).

The geology of the area consists of Tertiary fine sediments of the Molasse underlain by fractured siltstone. Seismic measurements show that the layer of mostly non-consolidated sediments is about 2~~1~~00 m thick, except close to the catchment outlet, where the weathered siltstone is found at the depth of about 5 m. Soil core drillings in 2016-18 show that the predominant soil texture down to 7 m below the surface is silt loam. Based on double-ring infiltrometer measurements on 12 plots in our study area, Picciafuocco et al. (2019) determined a mean saturated hydraulic conductivity of 46.9 mm h-1 and 20.2 mm h-1 for the top soil in arable land and grassland, respectively. The contact to the lignite sequence is found at the depth of 4 to 36 m below the surface. This is a series of dry, low-conductivity, massive and compact lignite layers interbedded by layers of wet, high-conductivity, non-consolidated sediments with pebbles. Unpublished pumping test results indicate that these non-consolidated layers have a hydraulic conductivity 10-100 times higher than the overlaying silt loams. Based on a soil survey conducted in 2010, the predominant soil types in the top 1 m are Cambisols (57%), Kolluvislos (16%), Planoslols (21%). Glaysols (6%) occur close to the stream (Széles et al., 2018).

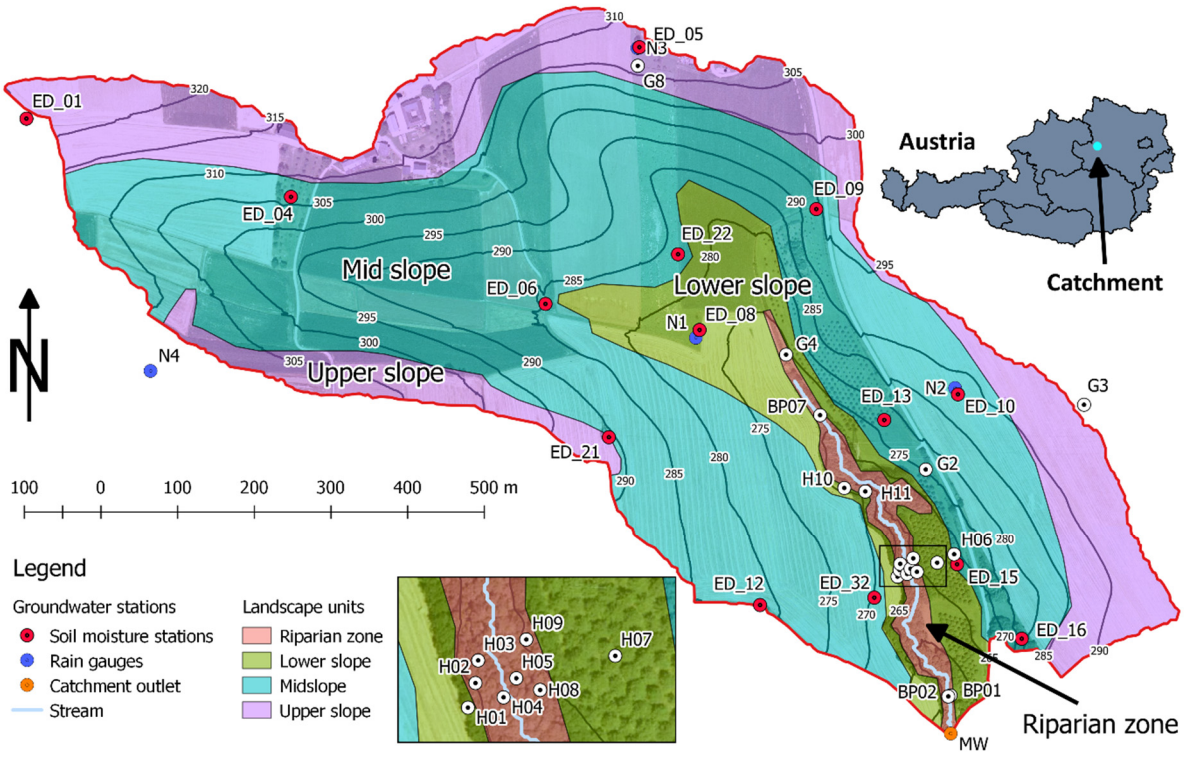

Figure 1: Hydrological Open Air Laboratory in Petzenkirchen, Lower Austria. Coloured areas represent different landscape units defined based on the Topographic Position Index, which compares the elevation of a point and the mean elevation of its surrounding. Elevation contours lines with a 5 m interval are given in black. The inset map is the detail of the area marked by a black rectangle on the main map.

In the HOAL catchment, a multitude of different runoff mechanisms are observed (Blöschl et al., 2016a). Exner-Kittridge et al. (2016) found that the stream baseflow is mostly due to diffuse groundwater flow directly to the stream or to the springs that feed the stream and partly due to the tile drainage discharge. During the rainfall events, saturation excess runoff and infiltration excess runoff occur in the valley bottom during prolonged or intensive rainfall events (Silasari et al., 2017). Part of the event water enters the stream as an overland flow but most infiltrates into the soil matrix and either percolates to the groundwater table or is routed to the stream via tile drains. Macropore flow is observed in summer when the topsoil dries and cracks up due to the high clay content (Exner-Kittridge et al., 2016). During rainless periods in the growing season, the diurnal fluctuations of transpiration by the riparian vegetation imprints a diurnal fluctuation on the streamflow, groundwater levels and soil moisture (Széles et al., 2018).

2.2 Data

There are four OTT Pluvio weighing rain gauges evenly distributed throughout the catchment (Fig. 1). They measure precipitation at 1 min intervals and the differences between the stations on the yearly scale do not exceed 5%. We use the arithmetic mean of precipitation amounts from all four stations as the representative precipitation for the whole catchment. Streamflow at the catchment outlet (MW) (Fig. 1) is routed through an H-flume and continuously measured by a Druck PTX1830 submersible pressure transmitter at a 1 min interval. There are 18 full days and 12 partial days of missing data in 2017-2018 due to measurement device or data transfer malfunction (Fig. 2).

We use the measurements from 18 groundwater measurement stations, of which 16 are in and around the forested area close to the stream and two are at the eastern and northern catchment boundary, respectively (Fig. 1, Table 1). The depth of the stations is between 1 and 41 m and they are screened along the whole depth. Most stations were drilled with a hammering rig to refusal which normally corresponds to the depth of the first consolidated lignite layer. Exceptions are stations G2, G3, G4

and G8 which were drilled into but not through all the lignite layers. All of the~~m~~ stations are equipped with pressure water level loggers by vanEssen, with a typical accuracy of 0.5 cmH_2O, which measure at 5 min time intervals. Barometric compensation of the water pressures of the water level loggers is performed using the atmospheric pressure measured by Baro Diver by vanEssen located close to H11 (Fig. 1). Stations G3, G4 and G8 were only installed in February 2017 and G2 in July 2017 but they are used in the study due to their locations outside of the forested area. Other stations only have missing data from the 4th to the 7th of December 2018 due to measurement device failure (Fig. 2).

Table 1: Groundwater (GW) measurement stations in the HOAL used in this study. Distance to the stream and distance to the catchment outlet are the distances along the surface flow path from the GW station's location to the nearest stream reach and catchment outlet, respectively. TWI and TPI are the topographic wetness and topographic position indices, respectively. ~~Last~~ The last column shows the number of events when a response was observed.

Station	Landscape ~~Position~~Unit	Total depth [m]	Mean GW depth [m]	Distance to the stream [m]	Distance to the catchment outlet [m]	TWI [-]	TPI [-]	Local Slope [%]	Days without data	Number of event responses
BP01	riparian	1.12	0.29	1	55	12.89	-2.40	4.68	2	51
BP02	riparian	1.13	0.27	1	55	12.89	-2.15	7.75	2	34
BP07	riparian	1.59	0.47	1	565	12.57	-3.07	5.60	0	32
G2	mid slope	15.00	2.52	76	491	6.89	-0.19	10.21	186	31
G3	upper slope	15.00	10.54	330	620	7.81	0.38	0.20	52	0
G4	riparian	8.00	1.43	93	676	8.16	-1.55	7.87	110	27
G8	upper slope	41.00	28.94	588	1162	5.41	1.27	7.04	108	0
H01	lower slope	5.97	4.21	28	287	5.96	0.06	11.22	2	24
H02	riparian	2.95	2.64	12	295	6.15	-1.17	13.17	2	32
H03	riparian	3.70	0.36	7	296	10.40	-3.44	11.05	2	35
H04	riparian	3.50	0.39	1	276	12.68	-3.06	6.69	2	36
H05	riparian	3.89	0.17	10	282	13.03	-3.42	4.23	2	37
H06	mid slope	3.57	1.08	75	333	7.90	0.02	5.51	2	30
H07	lower slope	3.84	1.91	48	306	8.07	0.42	4.51	9	21
H08	riparian	2.90	1.75	7	281	8.12	-1.22	8.79	2	27
H09	lower slope	3.89	2.57	27	312	7.42	-0.63	10.01	2	14
H10	lower slope	4.87	3.04	23	474	7.01	-0.34	9.53	0	10
H11	lower slope	4.96	4.46	13	451	4.99	-0.05	14.06	0	17

The soil moisture monitoring network at the study site is equipped with Spade time-domain transmission sensors from Forschungszentrum Jülich, Germany, at four depths below the ground surface (5, 10, 20 and 50 cm)(Blöschl et al., 2016b). For this study, we use 12 permanent stations in the forest, orchards, meadows or field edges and 2 temporary stations in the fields (Fig. 1, Table 2~~Table~~). The temporary stations are removed and reinstalled twice a year following the agricultural practises in the fields. Data is collected at an hourly timestep and each sensor at each site is calibrated using the gravimetric soil samples. ~~When at least two of the four sensors at the station are working, w~~We obtain the average volumetric soil moisture over a depth of 60 cm following Eq. (1):

$$\theta = \sum_{i=1}^{4} \theta_i \frac{d_i ~~d_{i+1} - d_{i-1}~~}{~~2d_5~~ D}, \quad (1)$$

where θ is the mean volumetric soil moisture content; the θ_i is the volumetric soil moisture content at i-th sensor, D is the soil column depth (60 cm) and d_i~~i~~ is the column height ~~depth of~~ the i-th sensor is representative for ($d_{~~0~~1}$ to $d_{~~5~~4}$ are 0.75,

0.755, 10, 20, 50 and 6035 cm). If measurements from one or two sensors are missing the d_i-are adjusted so that working sensors represent more of the soil column depth.

Table 2 Soil moisture (SM) measurement stations and their properties. * denotes a temporary station. Distance to the stream and distance to the catchment outlet are the distances along the surface flow path from the SM station's location to the nearest stream reach and catchment outlet, respectively. TWI and TPI are the topographic wetness and topographic position index, respectively. Last The last column shows the number of events when a response was observed.

Station	PositionLandscape unit	Distance to the stream [m]	Distance to the catchment outlet [m]	TWI [-]	TPI [-]	Local Slope [%]	Days without data	Number of event responses
ED_01	upper slope	1250	1840	5.91	0.72	4.09	62	24
ED_04	mid slope	911	1476	6.08	0.28	8.17	316	36
ED_05	upper slope	613	1189	5.35	1.26	3.70	74	20
ED_06	lower slope	433	1012	11.56	-0.14	2.65	331	28
ED_08	lower slope	213	792	9.29	-0.43	2.35	44	22
ED_09	mid slope	353	927	6.72	0.25	11.28	41	14
ED_10*	mid slope	181	597	7.57	-0.31	4.48	22	33
ED_12	mid slope	238	533	6.00	0.64	4.14	161	35
ED_13	mid slope	91	569	7.29	-0.65	8.79	127	32
ED_15	mid slope	81	314	7.59	0.15	5.51	95	40
ED_16	mid slope	175	257	4.76	1.15	20.26	112	27
ED_21	upper slope	356	937	6.78	0.69	4.91	33	29
ED_22	mid slope	325	888	6.01	0.66	4.21	68	18
ED_32*	mid slope	61	290	6.74	0.43	7.12	51	16

For this study, we use the streamflow at the catchment outlet, groundwater levels, precipitation and soil moisture data from the years 2017 and 2018. We aggregate average the groundwater and streamflow data with the 5 min time-step to 15 min time step and linearly interpolate the soil moisture data from 1 hour to the 15 min time-step. This time-step is small enough to capture the quick responses of streamflow, groundwater, and soil moisture to the precipitation. The streamflow, groundwater levels and soil moisture data are additionally smoothed using the locally estimated scatterplot smoothing (LOESS) as implemented in the *stats* package in R programming language (R Core Team, 2018). This is done to smooth out the measurement noise and ease the peak detection, which is based on the search for time-steps in the time-series preceded by consecutive rising and succeeded by consecutive decreasing values. Smoothing might have shifted the peak time by one-time step in some cases, which we deem acceptable since the majority of the peak-to-peak lag times were in orders of hours (see section 3.1.1). For the analysis on the seasonal scale, we further aggregate the dataset to median weekly values to dampen the event dynamics. We choose weekly time-step as it is longer than any observed events.

2.3 Site-characteristics

To put groundwater and soil moisture responses into the spatial context of the catchment we derive various site characteristics based on the sites' position and the digital elevation model (DEM) with 1 m resolution smoothed with a 10 m by 10 m box filter. For the calculations, we use SAGA GIS (Conrad et al., 2015). First, local slope and general curvature of the topography are calculated. Upslope catchment area and surface flowpaths are determined from the DEM by the Multiple Flow Direction method (Freeman, 1991). The distance along the surface flowpath from each of the groundwater or soil moisture station to the nearest stream reach and the catchment outlet is then calculated. The topographic control on local drainage is quantified by the Topographic Wetness Index (TWI) (Beven and Kirkby, 1979) which is calculated by the SAGA wetness index (Böhner and Selige, 2006) module in SAGA GIS.

Slope position is quantified by the Topographic Position Index (TPI) (Weiss, 2001). This compares the elevation of a point and the mean elevation of its surrounding. Points in the valleys have negative and points on the ridges have positive TPI values. TPI can be used for the classification of the landscape into slope position units. We classify our study site with the TPI Based Landform Classification tool in SAGA GIS into four position classes: Riparian zone, Lower slope, Middle slope and Upper slope (Fig. 1), with mean TPI values of -2.0, -0.4, 0 and 0.5 and mean slope of 7.5, 5.0, 6.5 and 4.2 degrees, respectively.

2.4 Rainfall-runoff ~~E~~event definition and characterisation

We identify 53 rainfall-runoff events during 2017 and 2018 (Fig. 2) ~~by following five rules as follows~~that meet all of the following six conditions: (1) Significant rainfall is more than 0.1 mm in 15 min; (2) Rainfall events are separated by a period of at least 6 hours when no significant rainfall occurs; (3) ~~The~~A rainfall event must have the rainfall depth of ~~must be~~ at least 4 mm; (4) The rainfall-runoff event starts with the rainfall event but continues after the rainfall has stopped for a recession period of 48 hours or until new rainfall event with a rainfall depth of at least 1 mm starts. ~~is a rainfall event extended by 48 hour recession period or to the start of the next rainfall event when at least 1 mm rainfall occurs~~Selected recession time covers most of the groundwater event dynamics while minimizing the coverage of the stream baseflow fluctuations; (5) No threshold is imposed on streamflow, however, no streamflow data ~~is~~should be missing during the duration of the rainfall-runoff event; (6) At least one groundwater or soil moisture response is found (Section 2.5).

For each event, we calculate the following event characteristics: the event duration is the total time between the start and end of the event as defined above. Rainfall event duration is calculated as time elapsed from the beginning of the event until 90% of the rainfall amount fell. Rainfall depth is the sum of all precipitation that occurred during the event. The maximum rainfall intensity is the maximum rainfall amount per 15 min interval during the whole event. Change in streamflow (dQ) is the difference between the maximum and minimum streamflow during the event. The streamflow peak time is the elapsed time from the beginning of the event until streamflow reaches its maximum. The runoff depth is the sum of the streamflow, reduced by its minimum, multiplied by the time step (15 min) and divided by the catchment area (66 ha). Following Saffarpour et al. (2016) we use antecedent soil moisture index (ASI) as the measure of antecedent catchment wetness. We calculate it as the mean volumetric soil moisture content of all soil moisture stations over 24 hours before the start of an event multiplied by the soil column depth (0.6 m) A table of all events and their characteristics is given in the appendix (Table A1~~Table~~).

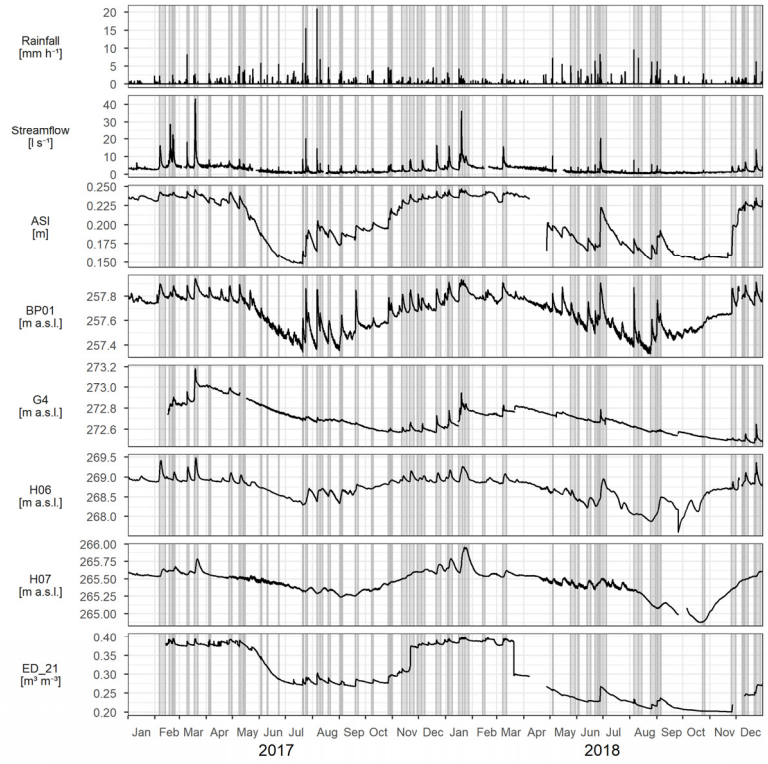

Figure 2: Dynamics of rainfall, streamflow at the catchment outlet, antecedent soil moisture index (ASI), groundwater (BP01, G4, H06, H07) and soil moisture (ED_21) during the investigation period, 2017–18. The shaded areas represent the times of analysed events.

2.5 Groundwater and soil moisture e~~E~~vent response definition and characterisation

We determine if the groundwater or soil moisture at a station reacted to the precipitation event based on the following rules: (1) stations' event time-series must not monotonously rise (Fig. 3b, station H06) or recede (Fig. 3b, station H07), must not be masked by a diurnal signal (Fig. 3b, station G4) and must have a peak (Fig .3a). The peak is a point in the time-series preceded by at least 24 time-steps of increasing and at least 4 time-steps of decreasing values. If more peaks are detected the one closest to the time of the streamflow peak is selected. (2) the minimum change in the groundwater table and soil moisture content is 5 mm and 0.005 m^3/m^3, respectively. The change is calculated as the difference of the value at the peak and the minimal value before the time of the peak. For each response, we also determine local antecedent conditions as the mean groundwater table or soil moisture one hour before the event.

During the 53 rainfall-runoff events, we observed a total of 458 groundwater responses to the precipitation at 15 stations and 374 soil moisture responses at 14 stations. For the comparison of these responses, we adopt three event descriptors: Spearman correlation coefficient, hysteresis index and peak-to-peak time. We choose these three because they are easy to understand, suitable for all variables whose responses are due to the same driver and they are transferable to other catchments.

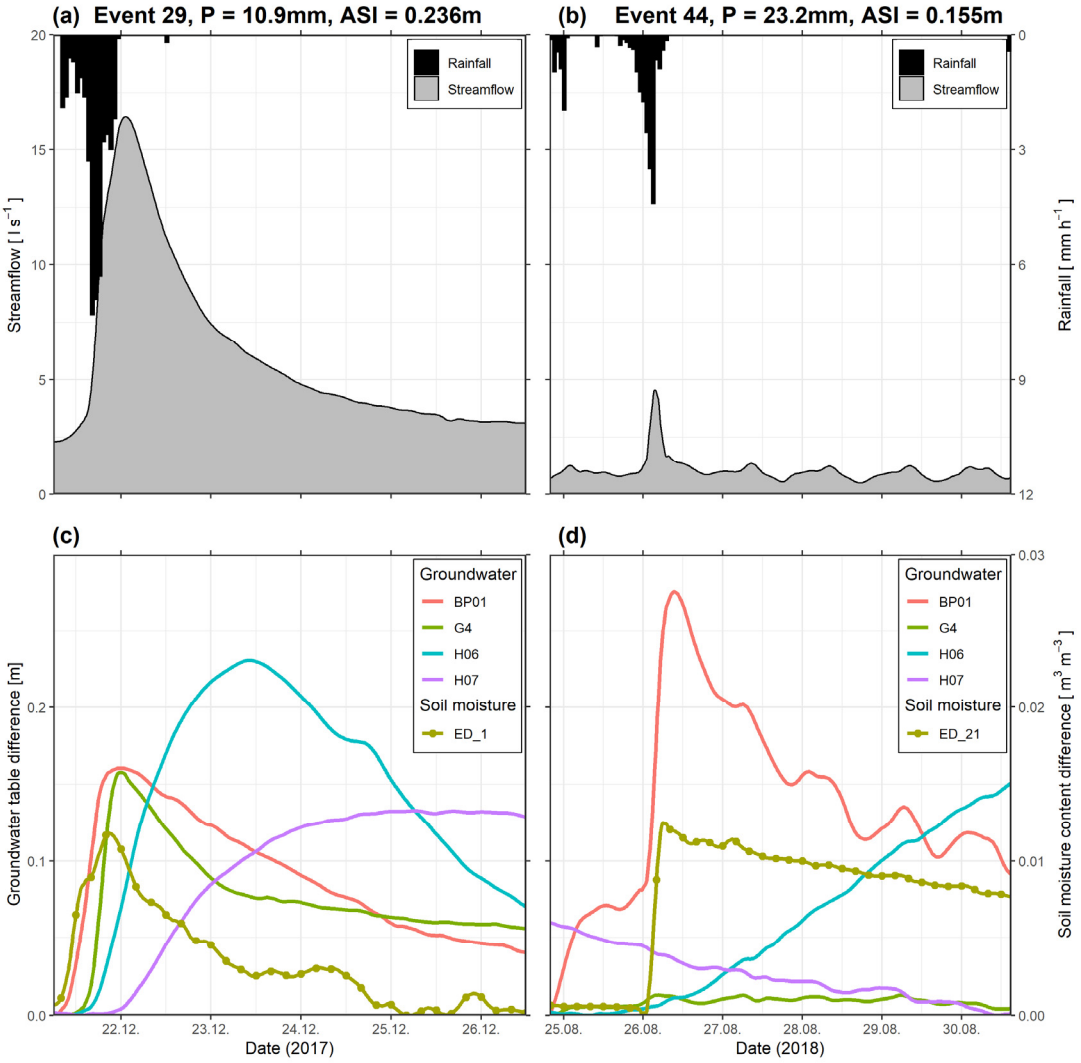

225 **Figure 3: Time-series of streamflow at the catchment outlet, rainfall (upper row) and groundwater table (BP01, G4, H06, H07) and soil moisture content (ED_21) (lower row) difference from the event minimum during event 29 (left column) and event 44 (right column). P and ASI denote the rainfall depth and antecedent soil moisture index of each of the events, respectively.**

Hysteresis loops have been demonstrated as a simple but insightful method for investigating the relationships between streamflow and other hydrological or chemical variables (Allen et al., 2010; Fovet et al., 2015; Scheliga et al., 2018). We can
230 obtain a hysteresis loop if we plot concurrent values of two variables, driven by the same driver, against each other. The hysteresis index (HI) describes the size~~shape~~ and rotational direction of such a loop. Various definitions of the HI have been proposed in hydrology (Aich et al., 2014; Langlois et al., 2005; Lawler et al., 2006; Lloyd et al., 2016; Zuecco et al., 2016). In this study, we use a definition similar to Lloyd et al. (2016) and Zuecco et al. (2016) in which the input data (e.g. streamflow, groundwater level, soil moisture) is normalized to values between 0 and 1 by the range of values for a specific
235 event~~:~~

~~$u(t) = \frac{x(t) - x_{min}}{x_{max} - x_{min}}$, (2)~~

~~$v(t) = \frac{y(t) - y_{min}}{y_{max} - y_{min}}$, (3)~~

~~where $x(t)$ and $y(t)$ are the two variables at time t and x_{min}, y_{min}, x_{max} and y_{max} their minimum and maximum values during the event; $u(t)$ and $v(t)$ are the normalized values of $x(t)$ and, $y(t)$, respectively, which range between 0 and 1~~. The
240 HI is then calculated as the integral of the curve enclosed by the two normalized variables plotted against each other. The resulting HI ranges between -1 and 1, where the magnitude describes the loop's shape and the sign the rotational orientation. The wider the loop the greater the absolute HI value. Clockwise loops, where the variable on the vertical axis~~x~~ peaks first~~lags behind y~~, have ~~negative~~ positive HI values and counter-clockwise loops, where the variable on horizontal axis~~y~~ ~~lags~~

~~behind~~peaks first, have ~~x, positive~~ negative HI values. A detailed explanation of the HI calculation can be found in Appendix B.

Peak-to-peak time is the time difference between the peak of the first and the peak of the second variable. Peak-to-peak times in relation to streamflow are positive if the streamflow peaks first and negative if the other variable peaks first.

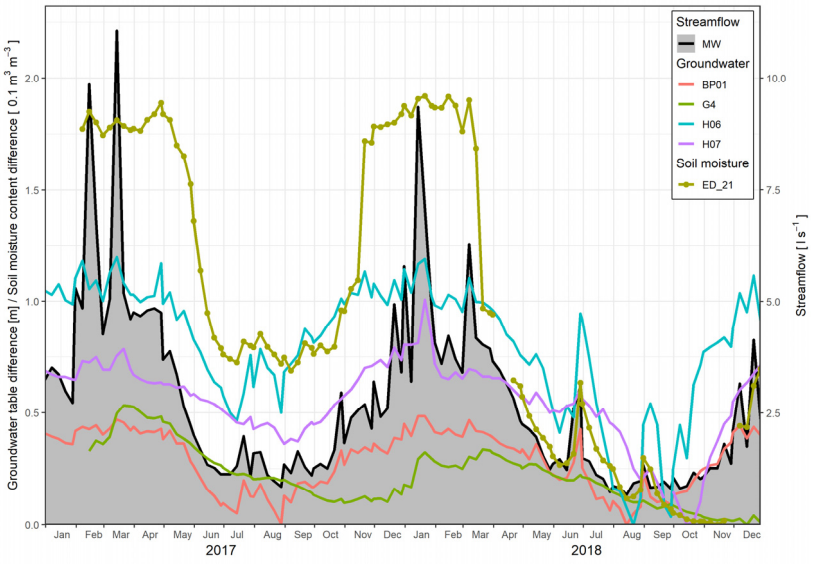

Figure 4: Weekly median time-series of streamflow at the catchment outlet (MW) and the groundwater table (BP01, G4, H06, H07) and the soil moisture content (ED_21) difference from the minimum for the years 2017–18.

To describe the similarity between streamflow, groundwater and soil moisture seasonal dynamics, we also use three descriptors~~Three descriptors are also calculated on the seasonal scale~~, i.e. Spearman correlation coefficient, hysteresis index and time shift in seasonal dynamics. Latter differs from the peak-to-peak time calculated on the event scale. It is determined using the cross-correlation between two time-series, i.e. the time-series time shift at which the Spearman correlation coefficient is highest is taken. For these calculations, the weekly median of streamflow, groundwater levels and soil moisture content are used to smooth out the event dynamics (Fig. 4). Only stations with more than 45 weeks of data in a year are used. Because of that station ED_32 is left out entirely, stations G2, G3, G4, ED_09 and ED_10 are left out for the year 2017 and stations ED_08 and ED_22 are left out for the year 2018.

For the analysis of spatial patterns, we calculated the median value of the three descriptors for each station pair over all events and both years. We investigate the temporal patterns in terms of changing wetness conditions, which can only be done on the event scale. For that, we use the comparisons of groundwater and soil moisture event responses to streamflow and aggregate them by landscape units and the sum of ASI and total rainfall. The entire analysis is done with R programming language (R Core Team, 2018). Statistical significance is assessed by p-values, which are calculated using the t-distribution approximation as implemented in the *stats* package in R.

2.6 Classification of event responses

To investigate the control of site- and event-characteristics on the connectivity on the event scale we first classify the relationship between the streamflow event response to the groundwater and soil moisture event response into response types, based on the event descriptors (Spearman correlation coefficient, hysteresis index and peak-to-peak time). For classification, we use a combination of the hierarchical clustering analysis and classification trees. An additional benefit of response types compared to the adopted descriptors is potentially better transferability to other catchments with for example more conductive soils. ~~The three adopted descriptors from the previous section are specific to the HOAL catchment and might not be transferable to other catchments with for example more conductive soils or longer concentration times. That is why we aggregate the relationship between the streamflow event response to the groundwater and soil moisture event response into response types, based on the event descriptors (Spearman correlation coefficient, hysteresis index and peak-to-peak time),~~

~~which are easily transferable. For the classification, We use a combination of the hierarchical clustering analysis and classification trees.~~

Hierarchical clustering is a method of identifying groups of similar data points in a dataset. Here we use above mentioned descriptors of groundwater event responses from all observed events at all available stations as the variables in the input dataset. Only groundwater responses are used because they have greater variability of descriptor values than soil moisture responses. The clustering is performed with Ward's hierarchical clustering algorithm (Murtagh and Legendre, 2014) implemented in *stats* package in R programming language (R Core Team, 2018), which gives us three clusters of similar size.

A disadvantage of hierarchical clustering is a lack of specific rules which could be used for classification of additional hydrological variables or datasets from other catchments. That is why we do an additional step and use the information gained from clustering to construct a discrete decision tree also known as a classification tree. The cluster number is used as a dependent and the three event descriptors are used as independent variables in the input dataset for the classification tree algorithm implemented in R package *rpart* (Therneau and Atkinson, 2019). The resulting three-node classification tree is shown in Fig. 5. It allows us to determine the type of relationship between two responses to the precipitation event, based only on the hysteresis index and Spearman correlation coefficient. The difference between the response type determined by the clustering and by the classification tree is less than 6%. This classification tree is also used here to classify the soil moisture responses to precipitation events in relation to streamflow.

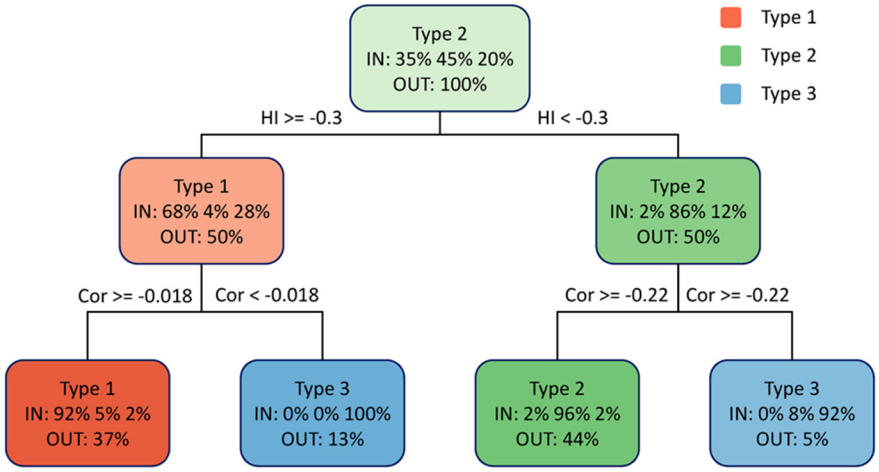

Figure 5: Decision tree for the classification of groundwater responses in relation to the streamflow responses to precipitation events into three response types. Responses are split based on the hysteresis index (HI) and Spearman correlation coefficient (Cor) as shown by the expressions on the horizontal lines between nodes. Each node is coloured based on the predominant response type, while the colour intensity denotes the purity of the classification. Node text shows the predominant response type, the percent of responses of each type at that node in the input database (IN) and the percent of the total number of responses at that node (OUT).

We assessed how site- and event-characteristics affect the connectivity on the event scale by looking at how they correlate with response types. We calculated the Pearson correlation coefficient between the frequency of each response type for each station to the site-characteristics and frequency of each response type for each event to the event-characteristics for groundwater and soil moisture stations, respectively. We deem correlations with $p < 0.05$ to be significant.

~~Altogether we determined 170, 203 and 85 groundwater responses and 136, 183 and 55 soil moisture responses in relation to the streamflow of Type 1, Type 2 and Type 3, respectively. Response types represent different levels of similarity between the groundwater or soil moisture to the streamflow, as follows:~~

Type 1 responses have a hysteresis index greater than -0.3 and Spearman correlation coefficient of more than -0.018. These were GW and SM responses that were similar to the streamflow response – the hysteresis loop was narrow, the lag time was short and GW table or SM content have increased and decreased on the same time scale as the discharge (Fig6a and d).

Type 2 responses had a HI less than -0.3 and correlation coefficient of more than -0.22. Typical for this response types are wide hysteresis loops. The rising limb of the GW/SM event hydrographs is relatively long but still overlaps with the rising and receding limb of the streamflow hydrograph (Fig. 6b).

Type 3 responses either had a HI greater than -0.3 and correlation coefficient lower than -0.018 or a HI lower than -0.3 and correlation coefficient lower than -0.22. These GW and SM responses were least correlated with streamflow. Their rising limb either started late after the start of the rainfall or continued to increase past the end of event time (Fig. 6c).

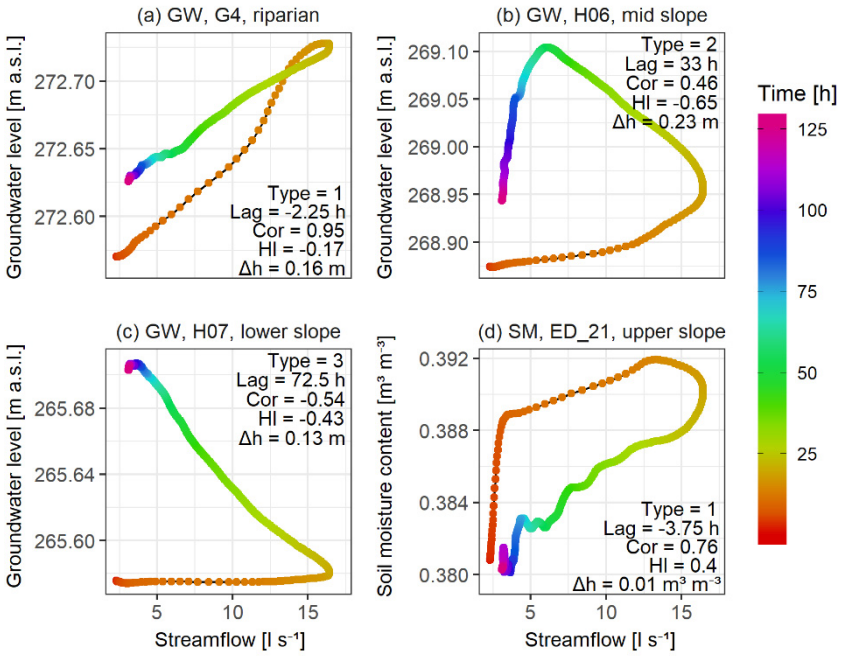

Figure 6: Hysteresis loops for the event 29 (2017-12-21) (Fig. 3, left column). Each panel represents different response type: (a) type 1 groundwater (GW) response; (b) type 2 GW response, (c) type 3 GW response; (d) type 1 soil moisture (SM) response. Colour of points represents the hours since the start of the event. Event dynamics of each station in relation to the streamflow is described by the response type (Type), peak-to-peak time (Lag), Spearman correlation coefficient (Cor), hysteresis index (HI) and groundwater table or soil moisture content change over the event (Δh).

3 Results

3.1 Similarity of groundwater, soil moisture and streamflow event responses

3.1.1 Spatial patterns ~~of similarity~~

We find spatial patterns in the median event Spearman correlation coefficients between groundwater responses and streamflow response (Fig. 6~~7~~). The riparian stations BP01, BP02, BP07, H04, H05 and G4 have the highest mean Spearman correlation to the streamflow ($r_s > 0.6$). Correlation is lower in other groundwater stations. All of the soil moisture stations have mostly moderate correlations to streamflow ($0.3 < r_s < 0.5$). The similarity among the stations in the same landscape unit is comparable to the similarity to streamflow. ~~Similar patterns exist among the stations in the same landscape units.~~ The riparian zone groundwater stations (Fig. 6~~7~~, red rectangle) have the highest Spearman correlation coefficients among them ($\overline{r_s} = 0.75$). Correlations among the lower slope and mid slope stations are lower and they are also not well correlated to other stations. Exceptions are station H11, which is positioned above the stream valley, but it is very close to the stream, and station G2, which is positioned far from the stream but in a constantly wet location. Overall, the soil moisture stations are well correlated among themselves ($\overline{r_s} = 0.69$) and moderately correlated with the riparian groundwater stations. Upper slope soil moisture stations have lower correlation among them and to other stations compared to the average for the soil moisture stations.

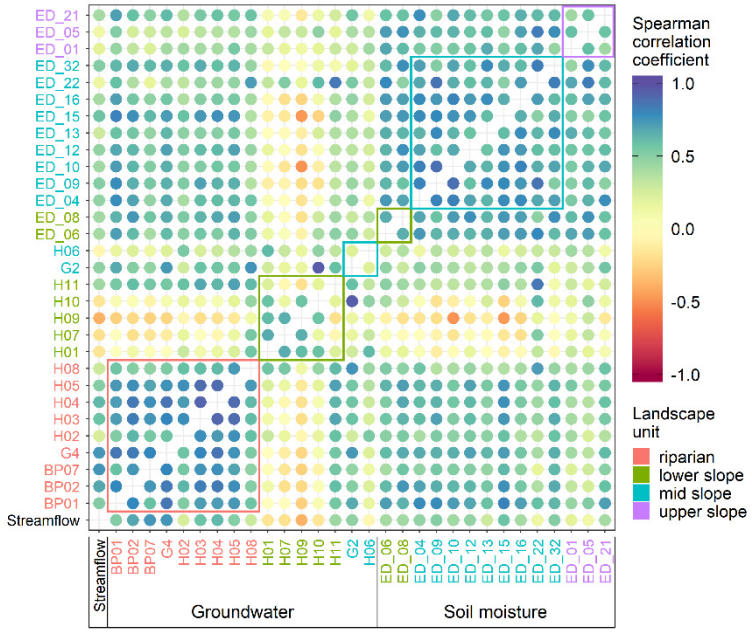

Figure 6~~7~~: Median Spearman correlation coefficient between streamflow at catchment outlet (Streamflow), groundwater stations (BP, H**, G*) and soil moisture stations (ED_**) for all events. Colour of the circles corresponds to the Spearman correlation coefficient; Colour of the station names corresponds to their landscape ~~position~~unit. Coloured rectangles enclose correlations of stations in the same landscape unit.**

The median event hysteresis indices between streamflow, groundwater and soil moisture event responses show similar spatial patterns (Fig. 7~~8~~) as the median event Spearman correlation coefficient. Where the Spearman correlation coefficient is high the hysteresis index is closer to zero and where the coefficient is low the absolute value of the hysteresis index is high. Most of the hysteresis indices of groundwater and soil moisture responses against streamflow responses are negative (Fig. 7~~8~~, first column) – indicating that on average the hysteresis loops are counter-clockwise and streamflow responds to precipitation, i.e. peaks (Fig. 8~~9~~, first column) and recedes, quicker than groundwater and soil moisture do.

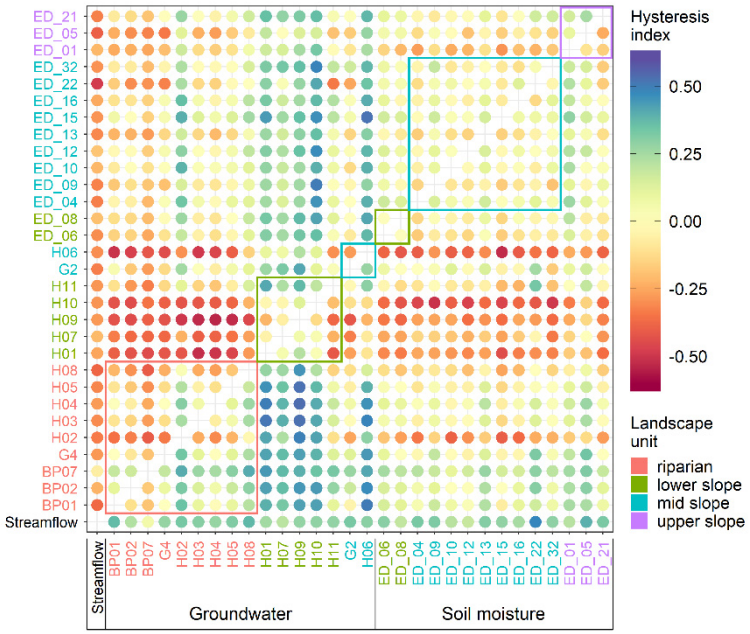

Figure 7~~8~~: Median hysteresis index between streamflow at catchment outlet (Streamflow), groundwater (BP, H**, G*) and soil moisture (ED_**) for all events. Hysteresis index is positive if the row station peaks before the column station and negative if the row station peaks after the column station. Colour of the circles corresponds to the value of the hysteresis index; Colour of the station names corresponds to their landscape ~~position~~unit. Coloured rectangles enclose values of stations in the same landscape unit.**

Spatial patterns in median event peak-to-peak times (Fig. 8~~9~~) confirm the assessment based on the hysteresis index (Fig. 7~~8~~, first column), that on average groundwater and soil moisture peak later than streamflow. Further, Fig. 8~~9~~ reveals details that are not so clearly visible in the median event correlation and hysteresis index. Upper slope soil moisture stations peak later than other soil moisture stations. We see also that stations H02 and H08 are different to the rest of the riparian stations and are more like the lower slope stations, which is probably due to their deeper groundwater table compared to the rest of the riparian stations.

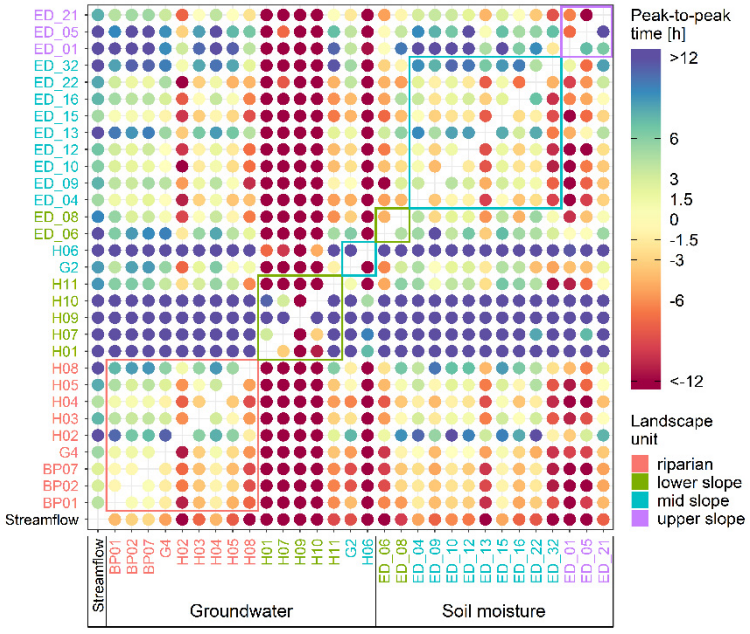

Figure 8~~9~~: Median peak-to-peak time between streamflow at catchment outlet (Streamflow), groundwater (BP, H**, G*) and soil moisture (ED_**). Time is positive if the row station peaks before the column station and negative if row station peaks after the column station. Colour of the circles corresponds to the value of the hysteresis index; Colour of the station names corresponds to their landscape ~~position~~unit. Coloured rectangles enclose values of stations in the same landscape unit.**

On average groundwater and soil moisture at all stations peak 15 ± 21 hours and 9 ± 14 hours (mean and standard deviation) after streamflow, respectively (Fig. 8~~9~~, first column). The lowest peak-to-peak times between streamflow and groundwater were observed in the riparian zone (median 2.7 ± 14 hrs), where in some instances groundwater even peaked before streamflow (Fig. A1c, Fig. 9f~~11 (c)~~). Pearson correlation coefficient between the event response Spearman correlation coefficient and TWI (Fig. A1a) and TPI is $\rho = 0.38$ and $\rho = -0.45$, respectively. Pearson correlation coefficient between the peak-top-peak time and TWI (Fig. A1c) and TPI is $\rho = -0.42$ and , $\rho = 0.51$, respectively. In other words, groundwater event responses towards the valley bottom where the contributing area is greater and the groundwater table is shallower are increasingly more similar to the streamflow responses and peak-to-peak times between them are decreasing. The soil moisture event response descriptors do not show any correlation to the site characteristics (Fig. A1).

3.1.2 Temporal ~~Similarity~~ patterns ~~change~~ through wetness conditions

While there is small spatial variability of descriptors for soil moisture responses in relation to the streamflow, the pattern changes in time with the catchment wetness (ASI + Rainfall depth) (Fig. 9~~10~~, top row). Spearman correlation coefficient and the hysteresis index increase with the increasing wetness (Pearson correlation of $\rho = 0.45$ and $\rho = 0.57$, respectively). The trend of peak-to-peak time is non-linear in the shape of an inverted parabola (Fig. 9~~10~~ c), with the longest times at medium wetness conditions. These three trends are very similar for all landscape units. The small dip in correlation and increase in peak-to-peak times during medium wetness conditions might indicate that different flowpaths activate during the dry and wet conditions.

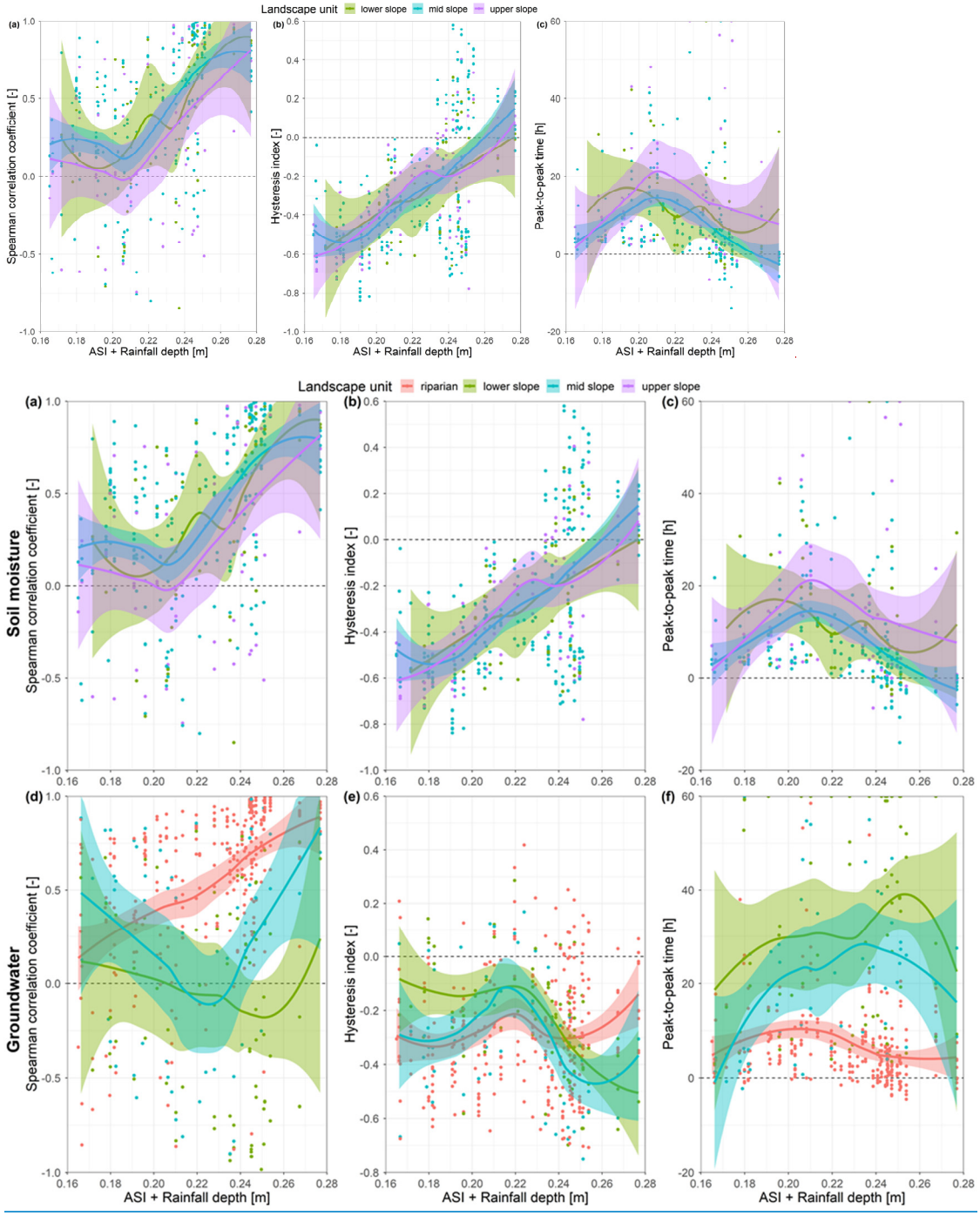

Figure 9~~10~~: Spearman correlation coefficient (a~~)~~ & d), hysteresis index (b~~)~~ & e) and peak-to-peak time (c~~)~~ & f) of soil moisture (top row) and groundwater (bottom row) responses to streamflow event responses over changing event catchment wetness conditions (ASI + Rainfall depth). Colours represent different landscape units. Points are calculated values for each available ~~soil moisture~~ response. Lines are local regression fits for each landscape unit and shaded areas the corresponding 95% confidence intervals.

Trends of groundwater event response descriptors with the wetness conditions differ for each landscape unit (Fig. 9, bottom row~~Fig. 11~~). Spearman correlation coefficient steadily increases with increasing wetness in the riparian zone (Fig. 9d ~~Fig. 11a~~), while there is no clear trend in the lower slope and a parabolic trend in mid slope, probably due to deeper groundwater table. Trends of hysteresis index and peak-to-peak time are not so clear. Peak-to-peak times are shorter in the riparian zone compared to other landscape units. They also seem to shorten with the increasing wetness, which is coherent with the increasing correlation. Peak-to-peak times in the mid slope are lower than in the lower slope, which is again coherent with the Spearman correlation coefficient. Trends of Spearman correlation coefficient and peak-to-peak time suggest that the control of the wetness conditions is related to the mean groundwater depth in the landscape unit. Trends are the clearest in the riparian zone where the groundwater table is the shallowest followed by the mid slope and lower slope, which has the deepest groundwater table.

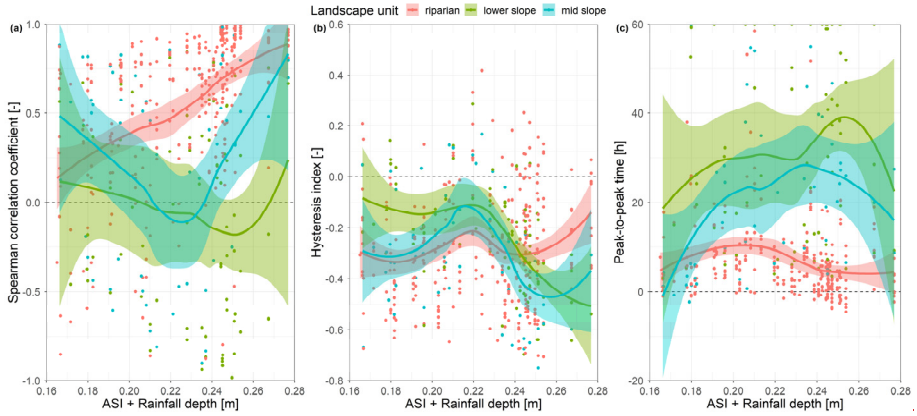

~~**Figure 11: Spearman correlation coefficient (a), hysteresis index (b) and peak-to-peak time (c) of groundwater responses to streamflow event responses over changing event catchment wetness conditions (ASI + Rainfall depth). Colours represent different landscape units. Points are calculated values for each available soil moisture response. Lines are local regression fits for each landscape unit and shaded areas the corresponding 95% confidence intervals.**~~

In the vast majority of cases groundwater peaks after the streamflow (Fig. 9~~Fig. 11~~). During wet conditions (ASI + Rainfall depth > 0.23) there is a more significant number of stations in the riparian zone that peak before. This probably indicates that most of the time event streamflow is fed by the flowpaths that bypass the groundwater (monitoring stations) and only when the catchment wetness is sufficiently high, the riparian zone contributes to the event streamflow.

3.2 Event ~~R~~response types ~~occurrence~~

3.2.1 Event response classification

Altogether we determined 170, 203 and 85 groundwater responses and 136, 183 and 55 soil moisture responses in relation to the streamflow of Type 1, Type 2 and Type 3, respectively. Response types represent different levels of similarity between the groundwater or soil moisture to the streamflow, as follows:

Type 1 responses have a hysteresis index greater than -0.3 and Spearman correlation coefficient of more than -0.018. These were groundwater~~GW~~ and ~~SM~~soil moisture responses that were similar to the streamflow response – the hysteresis loop was narrow, the lag time was short and groundwater ~~GW~~ table or ~~SM~~soil moisture content have increased and decreased on the same time scale as the discharge (Fig. 10a and d).

Type 2 responses had a hysteresis index~~HI~~ less than -0.3 and correlation coefficient of more than -0.22. Typical for this response types are wide hysteresis loops. The rising limb of the ~~GW/SM~~groundwater or soil moisture event time-series~~hydrographs~~ is relatively long but still overlaps with the rising and receding limb of the streamflow hydrograph (Fig. 10b).

Type 3 responses either had a ~~HI~~hysteresis index greater than -0.3 and correlation coefficient lower than -0.018 or a hysteresis index~~HI~~ lower than -0.3 and correlation coefficient lower than -0.22. These ~~GW~~groundwater and ~~SM~~soil moisture responses were least correlated with streamflow. Their rising limb either started late after the start of the rainfall or continued to increase past the end of event time (Fig. 10c).

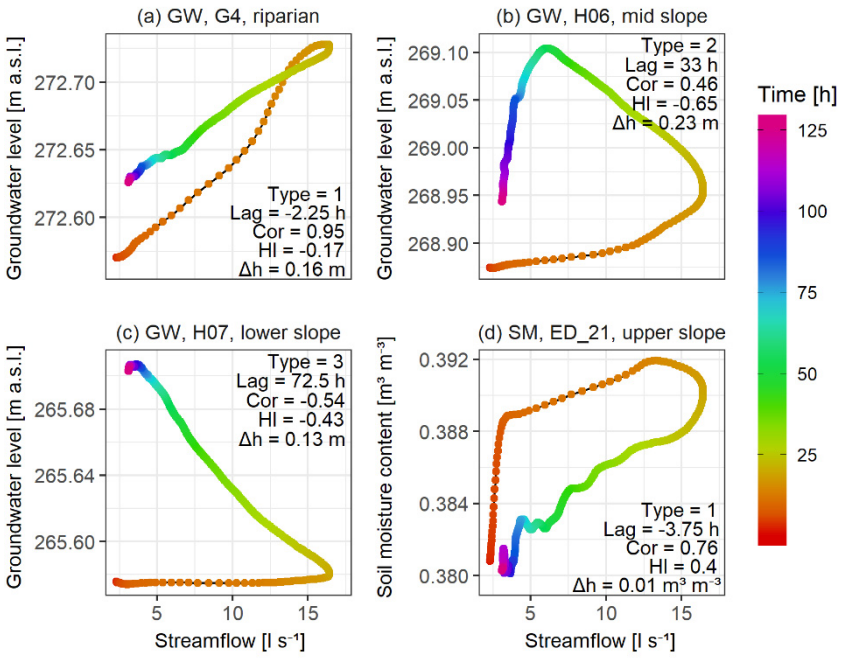

425 **Figure 10: Hysteresis loops for the event 29 (2017-12-21) (Fig. 3, left column). Each panel represents different response type: (a) type 1 groundwater (GW) response; (b) type 2 GW response, (c) type 3 GW response; (d) type 1 soil moisture (SM) response. Colour of points represents the ~~hours~~time since the start of the event. Event dynamics of each station in relation to the streamflow is described by the response type (Type), peak-to-peak time (Lag), Spearman correlation coefficient (Cor), hysteresis index (HI) and groundwater table or soil moisture content change over the event (Δh).**

~~3.1.3~~3.2.2 Spatial patterns of event response types

430 The spatial patterns of hysteresis index, Spearman correlation coefficient and peak-to-peak times (Section 3.1.1) propagate to the pattern of event response type ~~rate of~~ co-occurrence ~~of the same event response type between different stations~~ (Fig. 11~~12~~). Event response type co-occurrence is the frequency of events when two stations have the response of the same type. Apart from the riparian zone, where the co-occurrence rate is ~~0.~~64 % ± ~~0.~~15 % between stations, the other two landscape units show only low co-occurrence rates of groundwater response types between stations in the same unit. The highest 435 co-occurrence rate is observed between the three bank piezometers H03, H04 and H05. These stations respond with the same response type in more than 85 % of the events. Their co-occurrence rate with bank piezometers downstream (BP01, BP02) and upstream (BP07) is also high (~~0.~~68 % ~~—~~ ~~0.~~84 %), indicating that the distance to the stream is more important as the position along the stream. Riparian zone piezometers have a reasonable response type co-occurrence rate with the soil moisture stations (~~0.~~62 % ± ~~0.~~14 %). Soil moisture stations, with some exceptions, have high co-occurrence rates regardless 440 of the landscape ~~position~~ unit (mean ~~0.~~78 % ± ~~0.~~11 %).

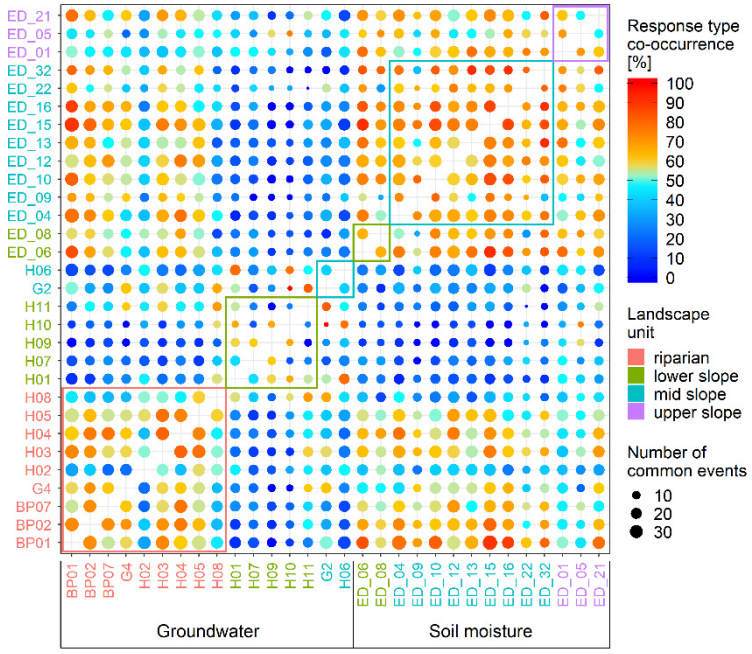

Figure 11~~12~~: The frequency of events when two stations have the response of the same type – i.e. response type co-occurrence. ~~Only events when both events have a response are considered – the number of such events is displayed by circle size~~The size of circles corresponds to the number of events when both stations had a response. Colour of the circles corresponds to the frequency of the response type co-occurrence. Colour of the station names corresponds to their landscape ~~position~~unit. Coloured rectangles enclose values of groundwater and soil moisture stations in the same landscape unit.

~~3.1.4~~3.2.3 Spatial and temporal controls of event response types

We observe the clearest trend in the groundwater response type frequency with the TPI and the TWI (Table 3~~Table~~). The frequency of the Type 1 responses decreases, and the frequency of the Type 3 responses increases with the increase of the TPI and the decrease in TWI (Fig. A2a). In both cases, this means that groundwater in the valley bottom reacts more similar to the streamflow than on the slopes and ridges. This is corroborated by the response type frequency against the stations' landscape ~~position~~unit. The Type 1 frequency is more than 43 % in the riparian zone and only 22 % and 18 % in the lower and middle slope, respectively. The highest frequency of Type 3 responses is at the lower slope (50 %), while it is the lowest in the riparian zone (7 %). The soil moisture response type frequencies do not vary considerably with the TPI or the TWI (Fig. A3a) but rather with the distance from the stream and catchment outlet and less pronounced with the terrain curvature and slope (Table 3~~Table 3~~). Soil moisture responses are less similar, i.e. frequency of Type 3 increases, further from the stream or catchment outlet and where the curvature and slope of the terrain are smaller.

Soil moisture response type frequencies are correlated the strongest with the catchment wetness (ASI, ASI + Rainfall depth) (Table 3~~Table 3~~). With increasing wetness, the similarity of soil moisture responses to the streamflow also increases (Fig. A3b). This correlation is weaker for the frequency of groundwater response types. The frequencies of both groundwater (Fig. A2c) and soil moisture (Fig. A3c) response types are correlated to the rainfall duration (Table 3~~Table 3~~). The responses are more similar to streamflow when the events are longer, i.e. less intensive.

Table 3 Pearson correlation coefficient of site- and event- characteristics to the frequency of different event response types of groundwater and soil moisture in relation to the streamflow. ASI is the antecedent soil moisture index. TPI and TWI are topographic position index and topographic wetness index, respectively. Significance of correlations was tested with t-distribution approximation and correlations with $p < 0.05$ are shown in bold.~~Values ≥ 0.4 and ≤ −0.4 are shown in bold.~~

		Groundwater responses			*Soil moisture responses*		
	Response type	**Type 1**	**Type 2**	**Type 3**	**Type 1**	**Type 2**	**Type 3**
Event characteristics	***ASI***	0.03	-0.03	**-0.38**	**0.67**	-0.24	-0.39
	ASI + Rainfall depth	0.09	-0.14	**-0.47**	**0.70**	**-0.38**	-0.40
	Rainfall duration	0.31	**-0.34**	**-0.40**	**0.47**	**-0.50**	-0.01

	Maximum rainfall intensity	-0.01	-0.17	0.32	**-0.39**	0.14	-0.03
	Rainfall depth	0.15	**-0.31**	-0.18	0.05	**-0.31**	0.03
Site characteristics	***Distance to the outlet***	0.35	-0.13	0.17	-0.24	-0.27	**0.59**
	Distance to the stream	0.03	-0.08	0.33	-0.11	-0.34	0.52
	Curvature	-0.29	0.31	-0.11	-0.09	0.26	-0.35
	Slope	-0.24	0.14	-0.02	0.11	0.28	-0.34
	Upslope area	0.36	0.18	-0.39	0.05	-0.01	-0.05
	TPI	**-0.57**	-0.31	**0.64**	-0.02	-0.08	0.10
	TWI	**0.56**	0.10	-0.48	0.10	-0.02	-0.09
	Mean groundwater depth	~~0.09~~0.43	~~**0.45**~~0.20	~~0.18~~-0.39	/	/	/

~~3.2~~3.3 ~~Seasonal responses~~Similarity of groundwater, soil moisture and streamflow seasonal dynamics

Examples of the seasonal hysteresis loops of the stations G4, H06, H07 and ED_21 are shown in Fig. 12~~13~~. Shapes of loops in panels A, B and C are different from corresponding event loops in Fig. 10~~6~~ indicating a difference in the similarity in the seasonal and the event dynamics of these stations to the streamflow. Further differences are seen when comparing the median seasonal Spearman correlation coefficients (Fig. 13~~14~~), hysteresis index (Fig. 14~~15~~) and time-shift (Fig. 15~~16~~) to their counterparts on the event scale (Figs. 6~~7~~, 7~~8~~ and 8~~9~~).

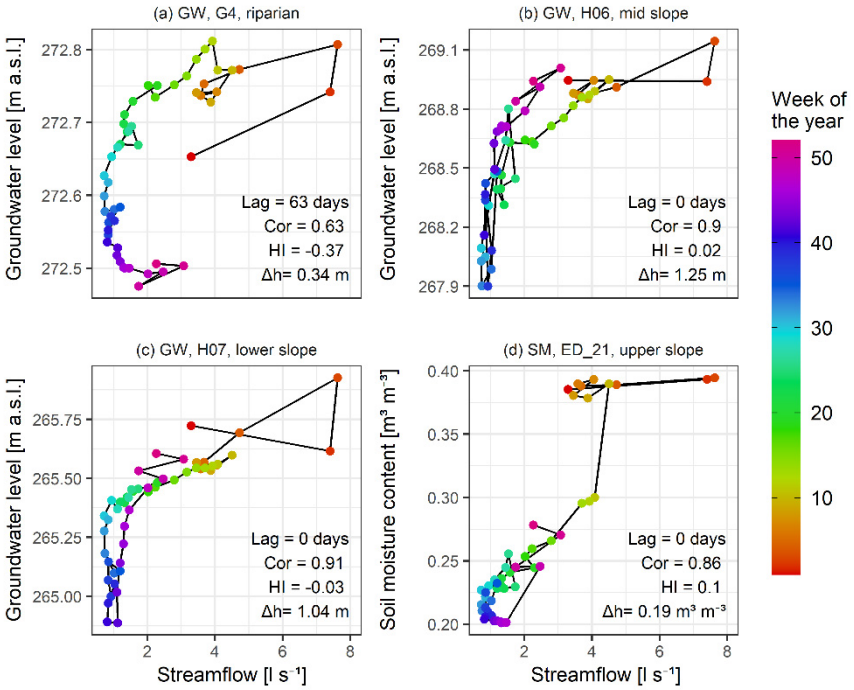

Figure 12~~13~~: Seasonal hysteresis loops of three groundwater stations (a, b, c) and one soil moisture station (d) to the streamflow for the year 2018 (Fig. 4). Colour of the points represents the ~~day~~ week of the year. Seasonal dynamics of each station in relation to the streamflow is described by time shift in seasonal dynamics (Lag), Spearman correlation (Cor), hysteresis index (HI) and groundwater table elevation or soil moisture content change over the year (Δh).

The Spearman correlation coefficient of groundwater and soil moisture seasonal dynamics to the streamflow (Fig. 13~~14~~) is, in contrast to the event scale, high ($\rho > 0.7$) for all stations except G2 ($\rho = 0.63$), G3 ($\rho = 0.14$), G4 ($\rho = 0.63$) and G8 ($\rho = 0.07$). Surprisingly, the lower and mid slope groundwater stations that have a low correlation to streamflow on the event scale show high correlation on the seasonal scale. Two examples are stations H01 and H06, with mean event correlation to streamflow of $\rho = -0.15$ and $\rho = -0.04$, and seasonal correlation of $\rho = 0.93$ and $\rho = 0.89$, respectively. Correlation among stations in the same landscape unit is the highest in the riparian zone also on the seasonal scale but the

difference to other units is smaller compared to the event scale. Even upper slope groundwater stations, which do not correlate well to stations in other landscape units, are well correlated to each other.~~Even upper slope groundwater stations which do not correlate to other stations are well correlated to each other.~~ All soil moisture stations are well correlated to the stream ($\overline{r_S} = 0.83 \pm 0.06$) and among them in all landscape units.

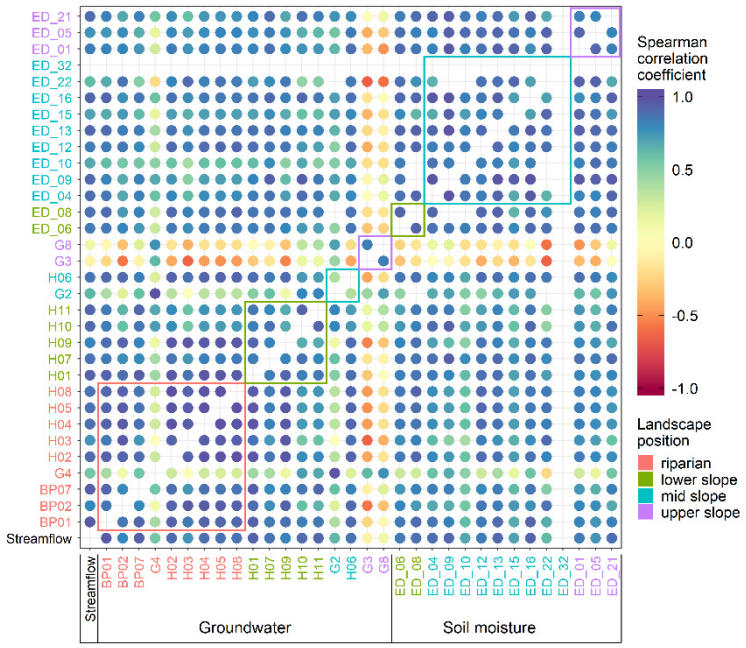

Figure 13~~14~~: Median Spearman correlation coefficient between median weekly streamflow at catchment outlet (Q), groundwater (BP, H**, G*) and soil moisture (ED_**) over years 2017 and 2018. Colour of the circles corresponds to the value of the Spearman correlation coefficient; Colour of the station names corresponds to their landscape ~~position~~unit. Coloured rectangles enclose values of stations in the same landscape unit. Only time-series longer than 45 weeks per year are compared.**

The pattern in the median seasonal hysteresis index (Fig. 14~~15~~) is more similar to the event pattern than the Spearman correlation coefficient. Riparian station G4 and some lower, mid and upper slope groundwater stations have negative hysteresis index against the streamflow (Fig. 14~~15~~, first column) indicating a delay in their seasonal dynamics. These are stations with the deepest groundwater table and some are also in contact with the deep groundwater system. All soil moisture stations have hysteresis index in relation to the streamflow close to zero or even slightly positive, indicating mostly synchronous seasonal dynamics.

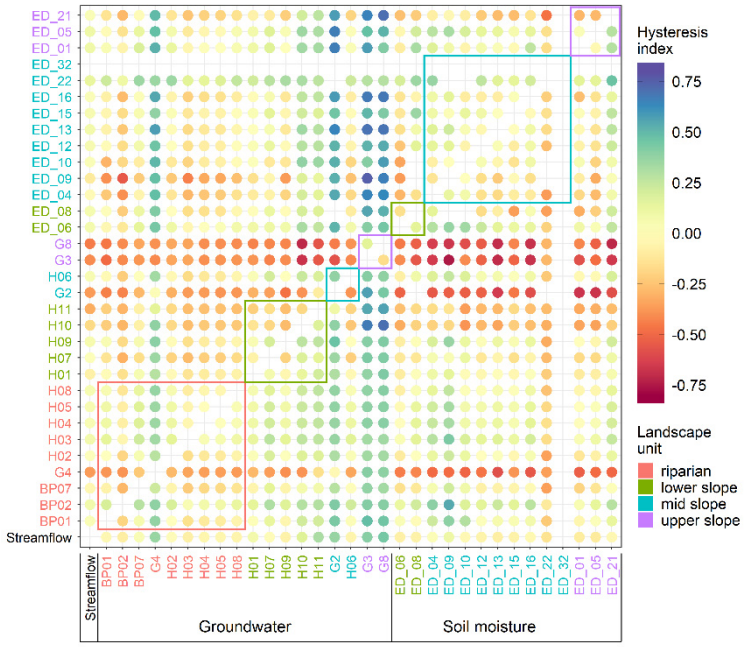

Figure 1415: Median hysteresis index between median weekly streamflow at catchment outlet (Q), groundwater (BP, H**, G*) and soil moisture (ED_**) over the years 2017 and 2018. Hysteresis index is positive if the row station peaks before the column station and negative if the row station peaks after the column station. Colour of the circles corresponds to the value of the hysteresis index; Colour of the station names corresponds to their landscape ~~position~~unit. Coloured rectangles enclose values of stations in the same landscape unit.**

Seasonal dynamics of streamflow, groundwater and soil moisture in the research area is roughly sinusoidal with highest values in winter and lowest in the summer. The seasonal dynamics shift time tells us how much out of phase are the dynamics of two stations. Fig. 1516 shows that the dynamics of stations G2, G3, G4 and G8 is delayed compared to the streamflow by 56, 91, 49 and 70 days, respectively. On the other hand, some soil moisture stations show slightly early dynamics, which indicates that soil moisture conditions drive the seasonal dynamics of streamflow and partly groundwater.

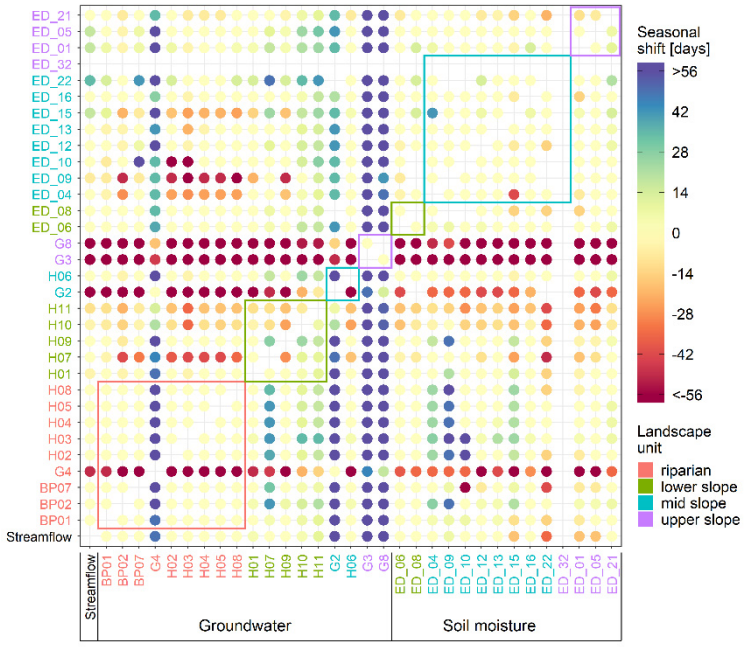

Figure 1516: Median seasonal shift between median weekly streamflow at catchment outlet (Q), groundwater (BP, H**, G*) and soil moisture (ED_**) over the years 2017 and 2018. The seasonal shift is positive if the row station's seasonal maxima and minima occur before the maxima and minima of the column station and vice versa. Colour of the dots corresponds to the value of the hysteresis index; Colour of the station names corresponds to their landscape ~~position~~unit. Coloured rectangles enclose values of stations in the same landscape unit. Only time-series longer than 45 weeks per year are compared.**

Spatial homogeneity of the seasonal soil moisture dynamics is reflected in a weak correlation between the site characteristics (Table 4~~Table 4~~) and the three descriptors, which is similar to what we also see on the event scale. Groundwater seasonal descriptors, on the other hand, are well correlated to most site characteristics. Distance to the stream has the highest correlation to all three descriptors, which is followed by the distance to the outlet and mean groundwater table depth. Spearman correlation coefficient between the groundwater and streamflow seasonal dynamics decreases with the increasing distance to the stream and the catchment outlet and depth to the groundwater table. In other words, stations closer to the stream with shallower groundwater table, i.e. riparian stations, have responses more similar to the streamflow, while stations on the catchment border with deep groundwater table, i.e. upper slope stations, are more different.

Table 4: Pearson correlation coefficient between site-characteristics and the Spearman correlation, hysteresis index and time shift of groundwater and soil moisture seasonal dynamics in relation to streamflow. TPI and TWI are topographic position index and topographic wetness index, respectively. Significance of correlations was tested with t-distribution approximation and correlations with $p < 0.05$ are shown in bold.~~Values ≥ 0.4 and ≤ -0.4 are shown in bold.~~

		Groundwater			*Soil moisture*		
	Descriptor	**Spearman correlation**	**Hysteresis index**	**Shift in dynamics**	**Spearman correlation**	**Hysteresis index**	**Shift in dynamics**
Site-characteristics	**Distance to the outlet**	**-0.69**	**-0.79**	**0.73**	0.03	0.02	-0.18
	Distance to the stream	**-0.87**	**-0.68**	**0.82**	0.04	0.00	-0.21
	Curvature	0.13	0.001	-0.05	-0.03	-0.05	-0.05
	Slope	**0.43**	0.06	**-0.37**	**0.34**	-0.25	0.23
	Upslope area	**0.26**	**0.34**	**-0.27**	0.04	0.08	0.17
	TPI	**-0.43**	**-0.54**	**0.46**	-0.08	0.04	-0.23
	TWI	**0.27**	**0.53**	**-0.34**	-0.03	0.06	0.16
	Mean groundwater depth	**-0.73**	**-0.65**	**0.69**	/	/	/

4 Discussion

4.1 Spatial and temporal patterns of groundwater and soil moisture responses to precipitation~~Spatial patterns of groundwater and soil moisture responses~~

In this study, we investigate patterns of the connectivity between streamflow, groundwater and soil moisture. We assess the connectivity as the similarity between two responses to the same precipitation event given by the Spearman correlation coefficient (Fig. 6~~7~~), hysteresis index (Fig. 7~~8~~), peak-to-peak times (Fig. 8~~9~~) and as all three aggregated into a response type (Fig. 11~~12~~). The similarity between different groundwater stations and between groundwater and streamflow event dynamics show spatial organisation related to the landscape units.

The highest similarity between the groundwater and streamflow event dynamics is observed in the riparian zone, where the groundwater table is closest to the surface and the soil water deficit is small throughout the year indicating that the riparian zone is constantly connected to the stream. Upslope from the stream, the similarity is lower (Figs. 6~~7~~ and 7~~8~~) suggesting lower connectivity to the stream than in the riparian zone. We attribute that to the deeper groundwater table compared to the riparian stations, based on the positive Pearson correlation of peak-to-peak times and the depth to the mean groundwater

table (Section 3.2.1). Greater groundwater depth equals to more available storage in the unsaturated zone and longer percolation path, both leading to later peak time. Another possible explanation for the lower connectivity upslope from the stream is that most water perched above the impeding lignite layer percolates through it before reaching the stream (Gabrielli and McDonnell, 2020; Klaus and Jackson, 2018).

Anti-clockwise hysteresis loops (Fig. 78 first column, Fig. 9cb) and positive peak-to-peak times (Fig. 89 first column, Fig. 9fe) between streamflow and groundwater event responses indicate that during the majority of events groundwater does not directly contribute to the event runoff or it does so only during the falling limb of the hydrograph. Event water, contributing to the rising limb of the hydrograph, probably bypasses the groundwater via surface flow, tile drains or other subsurface preferential pathways. Only riparian groundwater seems to contribute to the rising limb of the hydrograph, as it is suggested by the negative peak-to-peak times and positive hysteresis index (Fig. 9cb and fe) for some events (e.g. BP01 and G4 in Fig. 3a).

Other studies have found similar spatial patterns of groundwater event dynamics in humid headwater catchments. Haught and van Meerveld (2011) reported that streamflow and groundwater event responses were significantly better correlated in the footslope up to 8 m from the stream than in the hillslope further away from the stream. They concluded that strong correlation, together with small negative lag times suggest that transient groundwater in the lower hillslope contributes to event runoff. A similar difference between the riparian zone and the hillslope was reported by Scheliga et al. (2018) and Fovet et al. (2015). They observed mostly anti-clockwise hysteresis loops between streamflow and the deeper groundwater on the hillslopes and clockwise hysteresis loops in the valley bottom, reflecting the spatial difference in the availability of storage in the soils and groundwater system, which is high on the hillslope and lower in the riparian zone.

The similarity pattern changes with wetness conditions (Fig. 9). The similarity of groundwater to streamflow in the riparian zone increases with wetness. On the hillslope, the peak-to-peak times are the shortest and Spearman correlation coefficients are the highest during very dry and very wet conditions indicating the change in active flow paths. In summer months during dry conditions, the soils in the HOAL were observed to crack up (Blöschl et al., 2016a) enabling the water to infiltrate faster and during the wet conditions, the hydraulic conductivity increases due to the lower soil water deficit in both cases facilitating connectivity to the stream. Findings from other headwater catchments also suggest that groundwater connectivity to the stream increases with increasing catchment wetness. This could be manifested as the decrease of peak-to-peak lag times between hillslope groundwater and streamflow (Haught and Van Meerveld, 2011; Lana-Renault et al., 2014), higher groundwater peaks (Detty and McGuire, 2010) and fraction of activated wells (Penna et al., 2015).

We observed high variability of response dynamics between the lower and mid slope stations. Even stations just a few tens of meters apart, e.g. H04 and H02, could show different responses. This is in agreement with the short characteristic length scales of similarity found between the groundwater and streamflow event dynamics in a pre-alpine Swiss catchment (Rinderer et al., 2017). Also, groundwater event responses observed at the Bridge Creek Catchment in the Italian Dolomites could distinctly differ in magnitude and timing just a few meters apart (Penna et al., 2015).

We do not observe any spatial patterns in the similarity between the soil moisture and streamflow event responses and most of the soil moisture stations react similarly to each other (Fig. 1112). A reason for this homogeneity might be the small variability of topsoil texture (Blöschl et al., 2016a), local terrain slope and curvature (Table 2Table 2). However, we do find that the similarity with streamflow increases with increasing catchment wetness conditions (Fig. 910). Still, most of the hysteresis indices are negative (anti-clockwise) and the soil moisture peaks later than streamflow. Greater wetness corresponds to less available storage for the event water and increases hydraulic conductivity allowing faster percolation and redistribution of water and with that increasing the connectivity of the hillslope and the stream. Similar results were also reported by Penna et al. (2011) who also found that the relationship between streamflow and soil moisture responses in an Alpine catchment changed with wetness conditions. During dry conditions, they observed that streamflow started to rise and peaked before the soil moisture causing a clockwise hysteresis loop and during the wet conditions the soil moisture and

streamflow response were more synchronous with occasional anti-clockwise hysteresis loops. McGuire and McDonnel (2010) also observed a change in direction of the hillslope-streamflow hysteresis pattern with the increasing wetness conditions.

4.2 Dominant controls on the similarity between streamflow and groundwater or soil moisture ~~event responses~~dynamics

We classified the groundwater and soil moisture event responses based on similarity to streamflow as described by the Spearman correlation coefficient, hysteresis index and peak-to-peak time. The three classes represent three decreasing orders of similarity, which could also be interpreted as orders of connectivity. Type 1 responses are most similar to streamflow responses therefore we termed them "connected" responses. Processes governing the type 2 responses are slower than runoff generating processes but still on the time-scale of the event ~~therefore~~, therefore, we termed them "delayed" responses. Type 3 responses are least similar to streamflow and are too slow to contribute to the event streamflow. We ~~therefore~~, therefore, termed them "disconnected" responses. The response type is controlled by a mix of site and event-characteristics, which differ for groundwater and soil moisture.

Our analyses show that the similarity of groundwater event responses to streamflow is best correlated with the time-invariable site-characteristics (Table 3~~Table~~). The highest similarity is found for stations with the largest upslope area, high TWI, low TPI and gentle slope, which is typical for the riparian stations. These sites are typically close to the stream and have shallow groundwater table due to the lower gradient and large flux from the upslope so that only small amounts of rainfall are needed for groundwater to respond (Rinderer et al., 2017). On the other hand, upslope where the terrain is steeper and the upslope area is smaller, the TWI is lower and TPI is higher, the event groundwater dynamics is less similar to streamflow. The peak-to-peak times are longer and more variable in these sites compared to the riparian zone (Fig. 9f), most likely due to the thicker soils. The low similarity of hillslope sites to the streamflow suggests that these sites are less likely to connect to the stream and if so, mostly contribute to the falling limb of the streamflow hydrograph (Rinderer et al., 2017).

Other studies have also reported a strong correlation between the landscape ~~position~~ unit and the correlation between the groundwater and streamflow event dynamics in humid headwater catchments (Haught and Van Meerveld, 2011; van Meerveld et al., 2015; Rinderer et al., 2016, 2017; Rodhe and Seibert, 2011). Distance to the stream or the catchment outlet was found as the dominant control on the correlation between the transient water table and streamflow in the forested catchment in British Columbia (Haught and Van Meerveld, 2011). On the contrary, Rinderer et al. (2017) found that in a Swiss pre-Alpine catchment, the TWI explains more of the variability in the similarity between groundwater and streamflow than either distance to the stream or the catchment outlet, which is in good agreement with our findings.

Furthermore, we find that the event characteristics are less important controls on the similarity between groundwater and streamflow responses (Table 3~~Table 3~~). The highest correlation is found with the rainfall duration. Groundwater responds more similarly to streamflow during longer events. This suggests that flowpaths during the short and long events differ. Relatively low correlation to other event characteristics implies that the flow paths do not change significantly for different intensities and magnitudes of the rainfall events. Even during high-intensity summer and spring events when infiltration excess overland flow can occur on the western hillslopes (Blöschl et al., 2016a), the water would either be routed to the drainage pipes or infiltrate closer to the riparian zone where the terrain flattens. Both would not have a major impact on the groundwater responses at our measurement stations. Independence of the GW response from the rainfall intensity was also reported by Penna et al. (2015) and Dhakal and Sullivan (2014).

Controls on the similarity between the soil moisture and streamflow event responses are different than for the groundwater (Table 3~~Table 3~~). The topographic indices and upslope area are the weakest controls, while catchment wetness and rainfall duration are the strongest. The similarity increases with increasing ASI (+ rainfall depth) and rainfall duration. Distance to the stream and the catchment outlet is the strongest controls of the site-characteristics followed by the terrain slope and

curvature. Rosenbaum et al. (2012) found that the rainfall intensity had the strongest influence on the evolution of spatial soil moisture patterns during the wetting period at the Wüstenbach test site in Germany, which is not the case at our site.

We find stronger correlations between groundwater site-characteristics and the similarity descriptors on the seasonal scale compared to the event scale (Table 4~~Table 4~~). The strongest controls on the similarity of groundwater and streamflow seem to be the mean groundwater table depth and distance to the stream and catchment outlet. This again highlights the importance of proximity and soil water deficit for the connectivity of groundwater to the stream, as was also found in other studies (Haught and Van Meerveld, 2011; Rinderer et al., 2017). The similarity of soil moisture and streamflow seasonal dynamics is generally high and doesn't show a spatial pattern (Figs. 13~~14~~, 14~~15~~ and 15~~16~~), which is also reflected in low correlation with all site-characteristics (Table 4~~Table 4~~). Negative seasonal time shift of soil moisture to streamflow means that streamflow seasonal dynamics lags behind the soil moisture dynamics. This suggests, that on the seasonal scale the amount of soil moisture, which is a measure of catchment wetness, should increase first before the streamflow increases. Hence the catchment wetness controls the seasonal streamflow, i.e. baseflow.~~Negative seasonal time shift of some stations suggests that soil moisture – i.e. catchment wetness - controls the stream baseflow.~~

4.3 How are event and seasonal dynamics related?

Comparison of the similarity between the groundwater and streamflow dynamics on the event and seasonal scale reveals some interesting insights. Combining the differences found in the event (Figs. 6~~7~~, 7~~8~~ and 8~~9~~) and seasonal patterns (Figs. 13~~14~~, 14~~15~~ and 15~~16~~), we can divide the stations into four groups:

1. Stations which are more similar to streamflow on the seasonal scale than on the event scale. These are mostly located in lower and mid slope (e.g. H07 and H06) and are only in contact with shallow groundwater system. Similarity on the event scale is low, probably due to slower flowpaths compared to those contributing to the streamflow. On the seasonal scale, streamflow is fed by the shallow groundwater. Hence, ~~the~~ seasonal dynamics is synchronous.
2. Stations which are more similar to the streamflow dynamics on the event scale than on the seasonal scale (e.g. G2 and G4). From the borehole drillings, we know these are in contact with both the shallow and the deep groundwater system. On the event scale, the shallow groundwater flowpaths contribute to the relatively quick but normally small response, which is similar to streamflow. But these event responses are smaller in amplitude compare to the underlying seasonal dynamics~~ The dominant dynamics is seasonal~~, which is driven by the deeper flowpaths. These are slow~~er~~, causing the seasonal dynamics to shift, and have a low correlation to the streamflow dynamics.
3. Stations which show ~~similarly~~comparably high similarity to the streamflow dynamics on the event and seasonal scale. These stations are mostly in the riparian zone (e.g. BP01 and BP07), which is constantly connected to the streamflow, i.e. have similar dynamics.
4. Stations which have low similarity to the streamflow on both the event and seasonal scale. These are stations where the groundwater table is deeper than 10 m (e.g. G3 and G8) and does not react to precipitation event or it reacts on a much longer time scale than the streamflow. The slow celerity of flowpaths also causes the seasonal dynamics to shift resulting in low correlation to the streamflow.

Previously, Exner-Kittridge et al. (2016) found that in the HOAL about 39% of the yearly stream baseflow was due to the net diffuse groundwater flow from the riparian zone and that they are positively correlated. This is consistent with the high seasonal correlation between streamflow and groundwater in the riparian and lower slope stations. ~~Similar conclusions in terms of flowpaths in this study area were also found by Exner-Kittridge et al. (2016). They reported that, based on nitrate concentration measurements, the baseflow water mostly comes from the deep groundwater system – 25% from springs and 40% from the diffuse groundwater flow to the stream.~~

5 Conclusion

This study has examined the spatial-temporal patterns of connectivity between streamflow, groundwater and soil moisture in the Hydrological Open Air Laboratory, an agricultural headwater catchment in Lower Austria. We assessed the connectivity as a similarity between time-series as described by Spearman correlation coefficient, hysteresis index and peak-to-peak time

or a combination of the three classified into response types. The similarity of groundwater to streamflow shows spatial organisation suggesting a decreasing degree of connectivity to the stream from the riparian zone up the hillslope. The soil moisture pattern is spatially more homogeneous and the similarity to streamflow increases with increasing wetness conditions. ~~The soil moisture similarity pattern is spatially more homogeneous but changes with catchment wetness conditions.~~

We found that site-characteristics are the dominant controls on the connectivity between the groundwater and the stream on both the event and seasonal scales. Topographic indices and depth to the groundwater table were especially good predictors, highlighting the importance of surface topography and soil depth for spatial connectivity. Event-characteristics are only the secondary control for groundwater but the primary control for the soil moisture similarity to streamflow. This shows that in a catchment with low conductivity soils, rainfall characteristics and wetness conditions mostly affect the infiltration and water movement in the topsoil, while their effect on deep percolation is smaller.

Comparison of the seasonal and event similarity patterns revealed that the connectivity might change depending on the temporal scale we choose. The riparian zone is well connected to the stream on both scales, while the hillslope groundwater is better connected on the seasonal scale. Differences in the similarity patterns of groundwater on different time scales allowed us to divide the groundwater stations into groups which relate to their interaction with the two subsurface systems. ~~Differences in the similarity give us an insight into the interaction between the two subsurface systems.~~ Where and when the connectivity occurs is essential for the management practices in an agricultural catchment, for example where it is safe to apply fertilizers or pesticides for them not to be flushed to the stream.

Appendix A

Table A1: Identified events in the years 2017-2018 and their characteristics. ASI is the antecedent soil moisture index.

ID	Start	End	Event Duration [h]	Rainfall duration [h]	ASI [m]	ASI + Rainfall depth [m]	Maximal rainfall intensity [mm h^{-1}]	Rainfall depth [mm]	Maximal streamflow [l s^{-1}]	Minimal streamflow [ls^{-1}]	Change in streamflow [l s^{-1}]	Runoff depth [mm]	Streamflow peak time
1	06/02/2017 00:00	13/02/2017 00:00	168.000	15.000	0.238	0.251	2.500	12.950	16.151	3.774	12.140	2.535	06/02/2017 23:00
2	21/02/2017 10:00	22/02/2017 01:00	15.000	6.750	0.239	0.246	3.500	7.450	21.607	7.976	13.827	0.754	21/02/2017 14:30
3	22/02/2017 01:00	24/02/2017 00:00	47.000	6.250	0.241	0.245	2.100	4.050	19.810	6.594	7.170	0.273	22/02/2017 08:45
4	09/03/2017 22:20	12/03/2017 00:00	49.667	3.500	0.237	0.250	12.500	13.100	13.644	4.792	9.282	0.666	10/03/2017 00:45
5	18/03/2017 07:40	22/03/2017 08:00	96.333	26.000	0.236	0.267	5.100	31.575	41.897	4.721	37.237	6.155	19/03/2017 13:00
6	03/04/2017 22:15	04/04/2017 17:15	19.000	5.500	0.230	0.242	4.500	12.200	7.569	4.312	3.185	0.129	04/04/2017 06:00
7	26/04/2017 23:00	30/04/2017 05:55	78.917	27.500	0.228	0.247	3.300	18.850	7.385	4.147	3.169	0.508	27/04/2017 08:15
8	08/05/2017 22:00	11/05/2017 00:00	50.000	8.250	0.222	0.235	9.700	13.625	7.351	3.138	3.614	0.217	09/05/2017 08:15
9	13/05/2017 07:55	14/05/2017 04:00	20.083	2.000	0.227	0.232	5.500	4.425	4.899	2.927	1.445	0.033	13/05/2017 11:15
10	02/06/2017 15:45	03/06/2017 18:00	26.250	0.250	0.188	0.195	23.100	7.225	3.490	1.480	2.298	0.161	02/06/2017 18:30
11	10/06/2017 00:50	10/06/2017 18:55	18.083	2.250	0.177	0.182	6.200	4.650	3.023	1.260	1.297	0.036	10/06/2017 06:00
12	23/06/2017 02:05	23/06/2017 19:00	16.917	0.750	0.158	0.165	11.200	7.325	3.869	0.757	2.429	0.043	23/06/2017 05:00
13	20/07/2017 18:35	21/07/2017 19:00	24.417	4.000	0.148	0.167	9.200	18.650	7.029	0.990	6.278	0.238	20/07/2017 23:15
14	24/07/2017 10:10	26/07/2017 06:35	44.417	2.750	0.157	0.182	36.800	24.150	12.549	0.365	10.899	0.238	24/07/2017 15:30
15	06/08/2017 05:45	09/08/2017 19:00	85.250	12.500	0.166	0.210	40.100	44.550	12.203	0.872	10.770	0.482	06/08/2017 08:15
16	10/08/2017 00:00	12/08/2017 18:00	66.000	21.000	0.194	0.208	17.700	14.150	5.137	1.175	3.800	0.100	10/08/2017 03:15
17	19/08/2017 05:25	21/08/2017 19:00	61.583	29.250	0.184	0.207	5.100	22.250	4.277	0.828	3.375	0.151	19/08/2017 11:30
18	01/09/2017 13:40	02/09/2017 11:00	21.333	1.750	0.173	0.179	4.900	5.875	2.765	1.154	1.593	0.025	01/09/2017 17:30
19	03/09/2017 00:40	04/09/2017 19:00	42.333	10.750	0.174	0.192	5.500	17.550	4.065	0.700	2.831	0.162	03/09/2017 08:15
20	19/09/2017 04:10	22/09/2017 16:00	83.833	21.000	0.180	0.206	3.900	25.550	4.584	1.247	3.278	0.353	20/09/2017 02:30
21	08/10/2017 04:05	09/10/2017 20:50	40.750	18.000	0.194	0.201	8.000	7.200	2.647	1.264	1.327	0.050	09/10/2017 02:45
22	27/10/2017 04:25	28/10/2017 23:35	43.167	11.000	0.195	0.213	10.100	18.225	4.608	1.767	3.140	0.262	27/10/2017 18:15
23	28/10/2017 23:40	30/10/2017 09:25	33.750	10.500	0.207	0.220	8.000	12.475	5.123	1.689	3.431	0.318	29/10/2017 13:30
24	30/10/2017 09:30	01/11/2017 00:00	38.500	4.500	0.215	0.221	7.500	5.975	4.389	1.782	1.781	0.028	30/10/2017 12:30
25	11/11/2017 16:45	17/11/2017 17:55	145.167	25.000	0.222	0.239	4.200	17.100	5.085	1.502	3.492	0.551	12/11/2017 11:45
26	20/11/2017 16:45	25/11/2017 17:25	120.667	23.250	0.231	0.251	3.200	20.500	8.309	1.857	6.459	1.366	21/11/2017 21:00
27	29/11/2017 16:20	04/12/2017 03:00	106.667	14.000	0.230	0.241	1.600	10.975	3.120	1.809	1.358	0.154	30/11/2017 16:45
28	04/12/2017 03:05	08/12/2017 10:25	103.333	30.250	0.233	0.242	1.300	9.575	8.108	2.049	6.088	1.116	05/12/2017 14:30
29	21/12/2017 06:00	26/12/2017 12:00	126.000	11.750	0.236	0.247	2.100	10.925	16.423	2.293	14.126	2.617	22/12/2017 01:15
30	03/01/2018 07:55	04/01/2018 16:20	32.417	5.250	0.237	0.245	4.800	7.925	6.345	3.260	3.084	0.290	03/01/2018 15:00
31	04/01/2018 16:25	09/01/2018 00:00	103.583	8.500	0.241	0.254	2.900	13.075	16.034	3.733	11.813	1.517	05/01/2018 05:45
32	16/01/2018 07:30	21/01/2018 01:40	114.167	73.500	0.235	0.277	6.000	41.650	35.627	2.702	32.943	5.316	19/01/2018 09:45
33	07/03/2018 20:20	12/03/2018 09:25	109.083	2.250	0.230	0.237	4.000	6.675	15.098	4.402	10.835	1.754	08/03/2018 16:45
34	03/05/2018 23:50	05/05/2018 00:00	24.167	2.250	0.193	0.203	14.667	10.133	7.354	2.141	5.186	0.118	04/05/2018 03:30
35	24/05/2018 18:10	30/05/2018 00:00	125.833	6.000	0.186	0.196	14.400	9.433	3.389	0.791	2.166	0.165	25/05/2018 07:00
36	02/06/2018 08:20	03/06/2018 14:55	30.583	1.250	0.176	0.182	5.867	6.300	3.123	0.868	1.683	0.027	02/06/2018 11:45

ID	Start	End	Event Duration [h]	Rainfall duration [h]	ASI [m]	ASI + Rainfall depth [m]	Maximal rainfall intensity [mm h^{-1}]	Rainfall depth [mm]	Maximal streamflow [l s^{-1}]	Minimal streamflow [ls^{-1}]	Change in streamflow [l s^{-1}]	Runoff depth [mm]	Streamflow peak time
37	12/06/2018 15:35	17/06/2018 00:00	104.417	31.500	0.167	0.191	4.000	23.900	3.871	0.880	3.111	0.496	14/06/2018 02:15
38	22/06/2018 00:30	24/06/2018 22:30	70.000	17.000	0.168	0.182	7.733	13.767	4.572	1.007	3.556	0.073	22/06/2018 04:00
39	24/06/2018 22:35	26/06/2018 18:40	44.083	6.000	0.171	0.180	4.800	8.933	2.792	1.032	1.557	0.052	25/06/2018 04:00
40	26/06/2018 18:45	27/06/2018 14:50	20.083	4.750	0.172	0.178	3.733	5.300	2.678	1.117	1.574	0.057	27/06/2018 03:00
41	27/06/2018 14:55	05/07/2018 00:00	177.083	18.500	0.172	0.228	19.600	55.867	19.186	0.871	18.291	1.959	28/06/2018 10:15
42	05/08/2018 12:25	10/08/2018 15:55	123.500	3.000	0.163	0.180	38.100	16.825	5.673	0.000	5.320	0.235	05/08/2018 18:15
43	10/08/2018 16:00	14/08/2018 22:35	102.583	2.250	0.167	0.180	10.600	12.300	3.192	0.415	2.637	0.088	10/08/2018 19:15
44	24/08/2018 19:35	30/08/2018 15:00	139.417	30.250	0.155	0.178	13.500	23.225	4.558	0.493	3.919	0.175	26/08/2018 04:30
45	01/09/2018 12:35	02/09/2018 15:30	26.917	12.500	0.162	0.172	11.100	9.550	3.754	1.319	2.397	0.044	01/09/2018 15:45
46	04/09/2018 17:55	05/09/2018 18:00	24.083	2.750	0.186	0.192	4.100	5.525	2.289	0.752	1.132	0.044	04/09/2018 21:30
47	23/10/2018 16:05	26/10/2018 06:00	61.917	21.750	0.154	0.166	9.700	12.075	2.220	0.942	1.254	0.067	24/10/2018 17:15
48	25/11/2018 17:50	30/11/2018 16:30	118.667	26.500	0.160	0.196	2.400	35.975	4.481	1.231	3.121	0.426	26/11/2018 18:00
49	07/12/2018 23:45	08/12/2018 23:00	23.250	7.000	0.219	0.224	2.267	4.667	2.838	1.911	0.942	0.018	08/12/2018 04:30

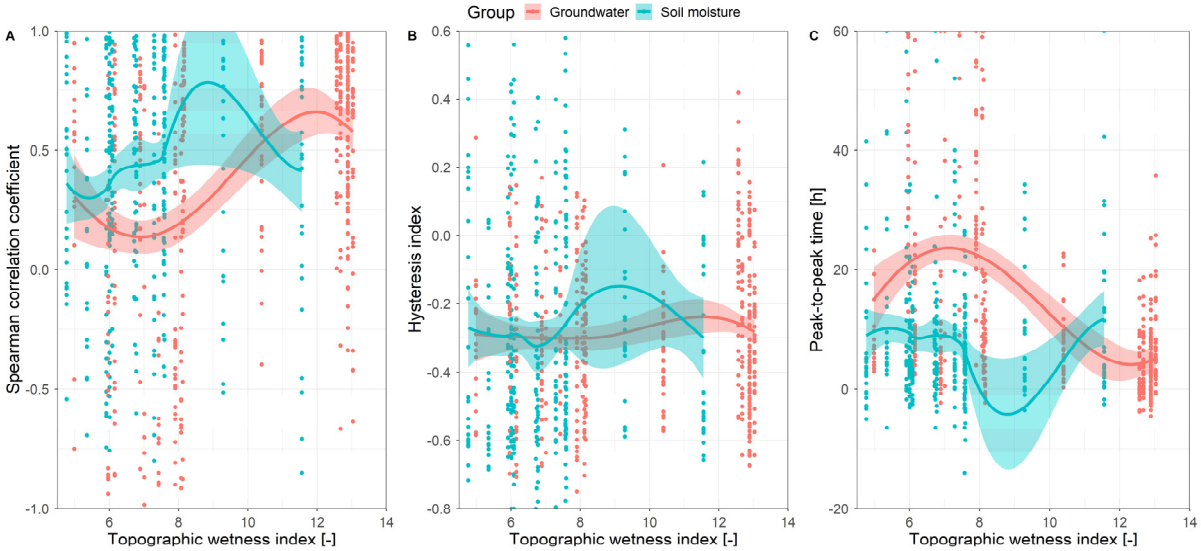

Figure A1: Spearman correlation coefficient (a), hysteresis index (b) and peak-to-peak time (c) of groundwater and soil moisture responses to streamflow event responses over locations with different topographic wetness indices. Colours represent different variable group, i.e. groundwater and soil moisture. Points are calculated values for a single event and station; lines are local regression fits for each variable group and shaded areas the corresponding 95% confidence intervals.

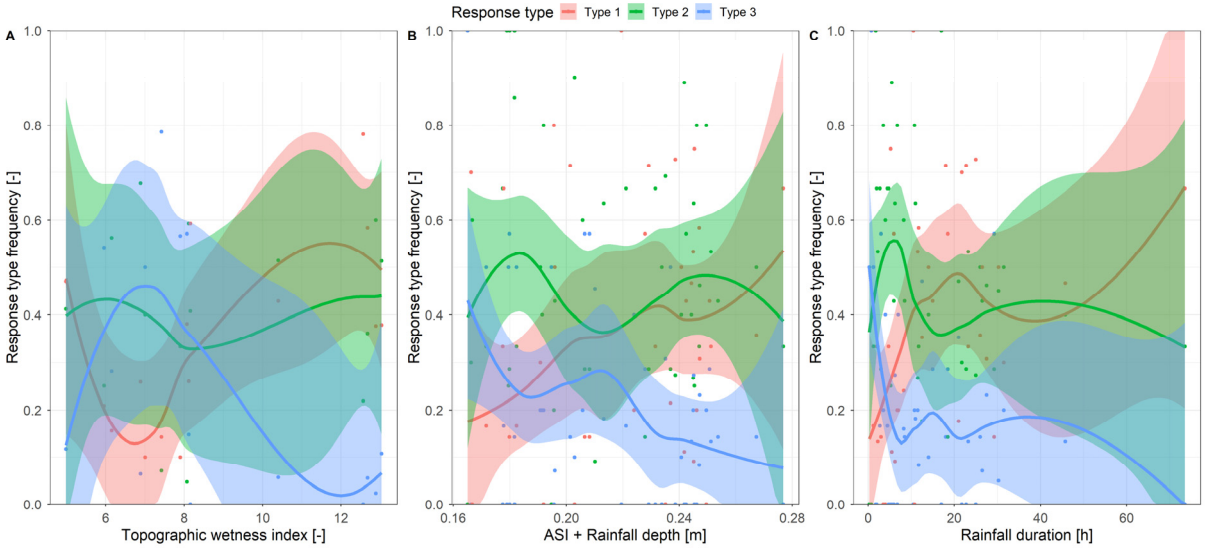

Figure A2: Groundwater response type frequency over stations topographic wetness index (a), a sum of antecedent wetness (ASI) and event rainfall depth (b) and rainfall event duration (c). Colours represent different response types as defined in section 2.6. Points are calculated values of response type frequencies; lines are local regression fits for each response type and the shaded areas corresponding 95% confidence intervals.

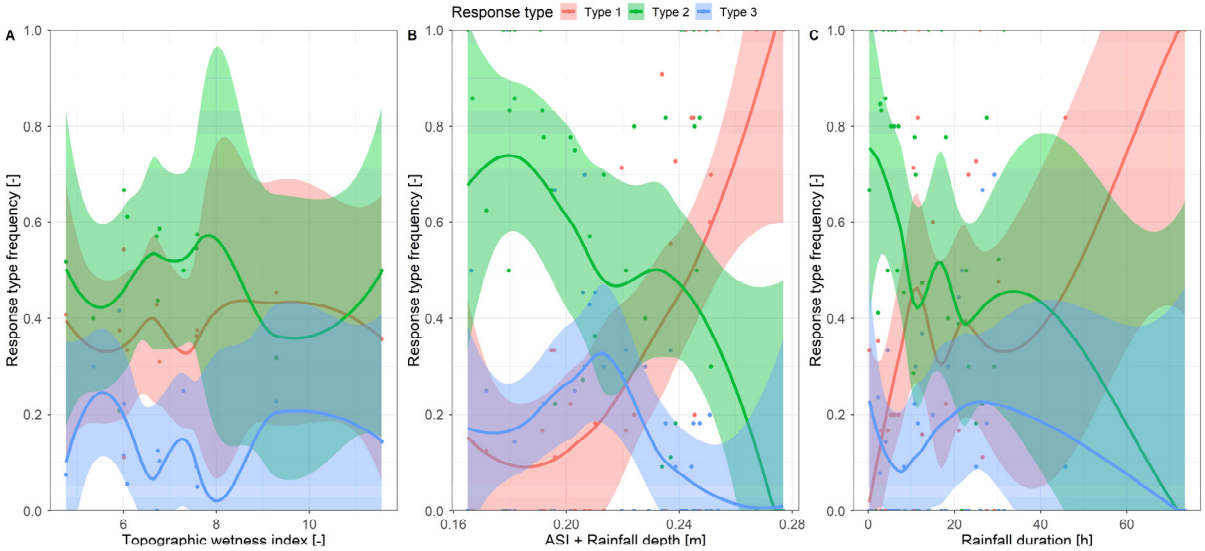

Figure A3: Soil moisture response type frequency over stations topographic wetness index (a), a sum of antecedent wetness (ASI) and event rainfall depth (b) and rainfall event duration (c). Colours represent different response types as defined in section 2.6. Points are calculated values of response type frequencies; lines are local regression fits for each response type and the shaded areas corresponding 95% confidence intervals.

Appendix B: Calculation of hysteresis index

Hysteresis index (HI) describes the size and rotational direction of a hysteresis loop. In this study, we use a calculation method similar to Zuecco et al. (2016). The calculation procedure is detailed below:

Let us have two time-series $x(t)$ and $y(t)$ spanning the same period and with the same time-steps, e.g. streamflow and groundwater responses to a precipitation event (Figure B1, a & b). First, the two time-series are normalized:

$$u(t) = \frac{x(t)-x_{\min}}{x_{\max}-x_{\min}}, \quad (1)$$

$$v(t) = \frac{y(t)-y_{\min}}{y_{\max}-y_{\min}}, \quad (2)$$

where x_{min}, y_{min}, $x_{\max}$ and $y_{\max}$ are the minimum and maximum values in the time-series $x(t)$ and $y(t)$, respectively; $u(t)$ and $v(t)$ are the normalized values of $x(t)$ and, $y(t)$, respectively, which range between 0 and 1. We then plot $v(t)$ against $u(t)$ to obtain a hysteresis loop (Figure B1 c).

We then calculate the HI by integrating the curve of the hysteresis loop. We do this here by using the trapezoidal rule, i.e. summing up the trapezoidal areas under the curve (Figure B1 d):

$$HI = \sum_{k=1}^{N} \frac{v(t_k)+v(t_{k+1})}{2} \left(u(t_{k+1}) - u(t_k)\right) \quad (3)$$

where N is the number of time-steps in the time-series and $v(t_k)$ and $u(t_k)$ are the values of the normalized time-series at the k-th time-step ($t_{N+1} = t_1$). Where the value of $u(t)$ is increasing ($u(t_{k+1}) - u(t_k) > 0$) the trapezoidal area has a positive contribution and where $u(t)$ is decreasing the area has a negative contribution to the index. This gives us a value of HI between -1 and 1. The HI is positive for clockwise loops, negative for counterclockwise loops and close to zero when there is no hysteresis or for symmetrical figure-eight loops or some complex shapes. The magnitude corresponds to the shape of the loop, i.e. the larger the loop, the closer the HI is to 1. The time-step used is arbitrary and can even vary as long as it is the same for both time-series and is fine enough to capture the observed processes. In contrast to the method of Zuecco et al. (2016), our method does not need the hysteresis loops to be split into a rising and a falling part. This makes it applicable to any complex shape of the loop, for example, a two-peak rainfall-runoff event where within one event streamflow rises and recedes two times. Nevertheless, results produced by our method are very comparable to the results of the method proposed by Zuecco et al. (2016).

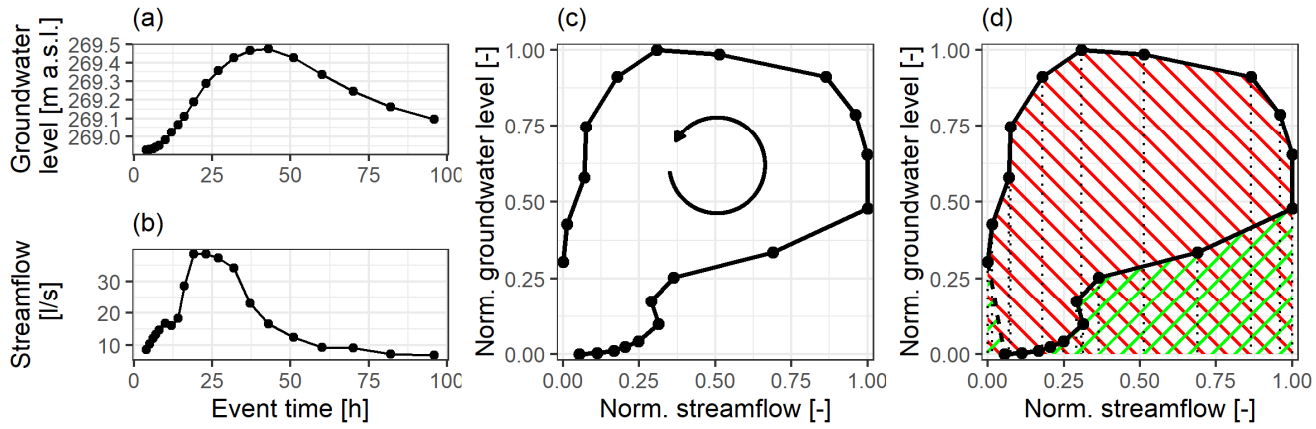

Figure B1: Example of the hysteresis index calculation: (a) and (b) show original groundwater and streamflow time-series, respectively; (c) shows the counterclockwise hysteresis loop of the normalized time-series from (a) and (b); (c) shows the positive and negative area contributions to the hysteresis index in green and red pattern, respectively. Hysteresis index is -0.64.

Data Availability

The data used in this study are available from the corresponding author upon request.

Author contribution

LP conceived and designed the study, performed the analyses and prepared the manuscript. BS collected and scrubbed part of the data used in the study. PS acquired part of the funding for the data collection. APB and GB contributed to the study design and interpretation of the results and acquired the funding for the project. All authors actively took part in the discussion of the results and revisions of the paper.

Competing interests

The authors declare that they have no conflict of interest.

Acknowledgements

The authors would like to acknowledge the financial support provided by the Austrian Science Funds (FWF) as part of the Vienna Doctoral Program on Water Resource Systems (DK W1219-N28).

Financial support

This research has been supported by the FWF Vienna Doctoral Programme on Water Resource Systems (grant no. W1219-N28).

References

Aich, V., Zimmermann, A. and Elsenbeer, H.: Quantification and interpretation of suspended-sediment discharge hysteresis patterns: How much data do we need?, Catena, 122, 120–129, doi:10.1016/j.catena.2014.06.020, 2014.

Allen, D. M., Whitfield, P. H. and Werner, A.: Groundwater level responses in temperate mountainous terrain: Regime

classification, and linkages to climate and streamflow, Hydrol. Process., 24(23), 3392–3412, doi:10.1002/hyp.7757, 2010.

Aubert, A. H., Gascuel-Odoux, C., Gruau, G., Akkal, N., Faucheux, M., Fauvel, Y., Grimaldi, C., Hamon, Y., Jaffrézic, A., Lecoz-Boutnik, M., Molénat, J., Petitjean, P., Ruiz, L. and Merot, P.: Solute transport dynamics in small, shallow groundwater-dominated agricultural catchments: insights from a high-frequency, multisolute 10 yr-long monitoring study, Hydrol. Earth Syst. Sci., 17(4), 1379–1391, doi:10.5194/hess-17-1379-2013, 2013.

Bachmair, S. and Weiler, M.: Hillslope characteristics as controls of subsurface flow variability, Hydrol. Earth Syst. Sci., 16(10), 3699–3715, doi:10.5194/hess-16-3699-2012, 2012.

Bachmair, S., Weiler, M. and Troch, P. A.: Intercomparing hillslope hydrological dynamics: Spatio-temporal variability and vegetation cover effects, Water Resour. Res., 48(5), 1–18, doi:10.1029/2011WR011196, 2012.

Beven, K. J. and Kirkby, M. J.: A physically based, variable contributing area model of basin hydrology, Hydrol. Sci. Bull., 24(1), 43–69, doi:10.1080/02626667909491834, 1979.

Blöschl, G., Blaschke, A. P., Broer, M., Bucher, C., Carr, G., Chen, X., Eder, A., Exner-Kittridge, M., Farnleitner, A. H., Flores-orozco, A., Haas, P., Hogan, P., Kazemi Amiri, A., Oismüller, M., Parajka, J., Silasari, R., Stadler, P., Strauss, P., Vreugdenhil, M., Wagner, W. and Zessner, M.: The Hydrological Open Air Laboratory (HOAL) in Petzenkirchen: A hypothesis-driven observatory, Hydrol. Earth Syst. Sci., 20(1), 227–255, doi:10.5194/hess-20-227-2016, 2016a.

Blöschl, G., Blaschke, A. P., Broer, M., Bucher, C., Carr, G., Chen, X., Eder, A., Exner-Kittridge, M., Farnleitner, A., Flores-Orozco, A., Haas, P., Hogan, P., Kazemi Amiri, A., Oismüller, M., Parajka, J., Silasari, R., Stadler, P., Strauss, P., Vreugdenhil, M., Wagner, W. and Zessner, M.: The Hydrological Open Air Laboratory (HOAL) in Petzenkirchen: A hypothesis-driven observatory, Hydrol. Earth Syst. Sci., 20(1), 227–255, doi:10.5194/hess-20-227-2016, 2016b.

Blume, T. and van Meerveld, H. J.: From hillslope to stream: methods to investigate subsurface connectivity, Wiley Interdiscip. Rev. Water, 2(3), 177–198, doi:10.1002/wat2.1071, 2015.

Böhner, J. and Selige, T.: Spatial prediction of soil attributes using terrain analysis and climate regionalisation, edited by J. Boehner, K. R. McCloy, and J. Strobl, Goettinger Geographische Abhandlungen, Goettingen., 2006.

Coles, A. E. and McDonnell, J. J.: Fill and spill drives runoff connectivity over frozen ground, J. Hydrol., 558, 115–128, doi:10.1016/j.jhydrol.2018.01.016, 2018.

Conrad, O., Bechtel, B., Bock, M., Dietrich, H., Fischer, E., Gerlitz, L., Wehberg, J., Wichmann, V. and Böhner, J.: System for Automated Geoscientific Analyses (SAGA) v. 2.1.4, Geosci. Model Dev., 8(7), 1991–2007, doi:10.5194/gmd-8-1991-2015, 2015.

Detty, J. M. and McGuire, K. J.: Topographic controls on shallow groundwater dynamics: implications of hydrologic connectivity between hillslopes and riparian zones in a till mantled catchment, Hydrol. Process., 24(16), 2222–2236, doi:10.1002/hyp.7656, 2010.

Dhakal, A. S. and Sullivan, K.: Shallow groundwater response to rainfall on a forested headwater catchment in northern coastal California: implications of topography, rainfall, and throughfall intensities on peak pressure head generation, Hydrol. Process., 28(3), 446–463, doi:10.1002/hyp.9542, 2014.

Emanuel, R. E., Hazen, A. G., Mcglynn, B. L. and Jencso, K. G.: Vegetation and topographic influences on the connectivity of shallow groundwater between hillslopes and streams, Ecohydrology, 7(2), 887–895, doi:10.1002/eco.1409, 2014.

Exner-Kittridge, M., Strauss, P., Blöschl, G., Eder, A., Saracevic, E. and Zessner, M.: The seasonal dynamics of the stream sources and input flow paths of water and nitrogen of an Austrian headwater agricultural catchment, Sci. Total Environ., 542, 935–945, doi:10.1016/j.scitotenv.2015.10.151, 2016.

Fovet, O., Ruiz, L., Hrachowitz, M., Faucheux, M. and Gascuel-Odoux, C.: Hydrological hysteresis and its value for assessing process consistency in catchment conceptual models, Hydrol. Earth Syst. Sci., 19(1), 105–123, doi:10.5194/hess-19-105-2015, 2015.

Freeman, T. G.: Calculating catchment area with divergent flow based on a regular grid, Comput. Geosci., 17(3), 413–422,

doi:10.1016/0098-3004(91)90048-I, 1991.

Gabrielli, C. P. and McDonnell, J. J.: Modifying the Jackson index to quantify the relationship between geology, landscape structure, and water transit time in steep wet headwaters, Hydrol. Process., 34(9), 2139–2150, doi:10.1002/hyp.13700, 2020.

Gannon, J. P., Bailey, S. W. and McGuire, K. J.: Organizing groundwater regimes and response thresholds by soils: A framework for understanding runoff generation in a headwater catchment, Water Resour. Res., 50(11), 8403–8419, doi:10.1002/2014WR015498, 2014.

Grayson, R. B., Western, A. W., Chiew, F. H. S. and Blöschl, G.: Preferred states in spatial soil moisture patterns: Local and nonlocal controls, Water Resour. Res., 33(12), 2897–2908, doi:10.1029/97WR02174, 1997.

Haught, D. R. W. and Van Meerveld, H. J.: Spatial variation in transient water table responses: Differences between an upper and lower hillslope zone, Hydrol. Process., 25(25), 3866–3877, doi:10.1002/hyp.8354, 2011.

Klaus, J. and Jackson, C. R.: Interflow Is Not Binary: A Continuous Shallow Perched Layer Does Not Imply Continuous Connectivity, Water Resour. Res., 54(9), 5921–5932, doi:10.1029/2018WR022920, 2018.

Lana-Renault, N., Regüés, D., Serrano, P. and Latron, J.: Spatial and temporal variability of groundwater dynamics in a sub-Mediterranean mountain catchment, Hydrol. Process., 28(8), 3288–3299, doi:10.1002/hyp.9892, 2014.

Langlois, J. L., Johnson, D. W. and Mehuys, G. R.: Suspended sediment dynamics associated with snowmelt runoff in a small mountain stream of Lake Tahoe (Nevada), Hydrol. Process., 19(18), 3569–3580, doi:10.1002/hyp.5844, 2005.

Latron, J. and Gallart, F.: Runoff generation processes in a small Mediterranean research catchment (Vallcebre, Eastern Pyrenees), J. Hydrol., 358(3–4), 206–220, doi:10.1016/j.jhydrol.2008.06.014, 2008.

Lawler, D. M., Petts, G. E., Foster, I. D. L. and Harper, S.: Turbidity dynamics during spring storm events in an urban headwater river system: The Upper Tame, West Midlands, UK, Sci. Total Environ., 360(1–3), 109–126, doi:10.1016/J.SCITOTENV.2005.08.032, 2006.

Lloyd, C. E. M., Freer, J. E., Johnes, P. J. and Collins, A. L.: Technical Note : Testing an improved index for analysing storm discharge – concentration hysteresis, , (1989), 625–632, doi:10.5194/hess-20-625-2016, 2016.

Loritz, R., Kleidon, A., Jackisch, C., Westhoff, M., Ehret, U., Gupta, H. and Zehe, E.: A topographic index explaining hydrological similarity by accounting for the joint controls of runoff formation, Hydrol. Earth Syst. Sci., 23(9), 3807–3821, doi:10.5194/hess-23-3807-2019, 2019.

McGuire, K. J. and McDonnell, J. J.: Hydrological connectivity of hillslopes and streams: Characteristic time scales and nonlinearities, Water Resour. Res., 46(10), doi:10.1029/2010WR009341, 2010.

van Meerveld, H. J., Seibert, J. and Peters, N. E.: Hillslope-riparian-stream connectivity and flow directions at the Panola Mountain Research Watershed, Hydrol. Process., 29(16), 3556–3574, doi:10.1002/hyp.10508, 2015.

Murtagh, F. and Legendre, P.: Ward's Hierarchical Agglomerative Clustering Method: Which Algorithms Implement Ward's Criterion?, J. Classif., 31(3), 274–295, doi:10.1007/s00357-014-9161-z, 2014.

Ocampo, C. J., Sivapalan, M. and Oldham, C.: Hydrological connectivity of upland-riparian zones in agricultural catchments: Implications for runoff generation and nitrate transport, J. Hydrol., 331(3–4), 643–658, doi:10.1016/J.JHYDROL.2006.06.010, 2006.

Penna, D., Tromp-Van Meerveld, H. J., Gobbi, A., Borga, M. and Dalla Fontana, G.: The influence of soil moisture on threshold runoff generation processes in an alpine headwater catchment, Hydrol. Earth Syst. Sci., 15(3), 689–702, doi:10.5194/hess-15-689-2011, 2011.

Penna, D., Mantese, N., Hopp, L., Dalla Fontana, G. and Borga, M.: Spatio-temporal variability of piezometric response on two steep alpine hillslopes, Hydrol. Process., 29(2), 198–211, doi:10.1002/hyp.10140, 2015.

Picciafuoco, T., Morbidelli, R., Flammini, A., Saltalippi, C., Corradini, C., Strauss, P. and Blöschl, G.: On the estimation of spatially representative plot scale saturated hydraulic conductivity in an agricultural setting, J. Hydrol., 570, 106–117, doi:10.1016/J.JHYDROL.2018.12.044, 2019.

R Core Team: R: A language and environment for statistical computing. R Foundation for Statistical Computing, Vienna, Austria, 0, 201, doi:10.1108/eb003648, 2018.

Rinderer, M., van Meerveld, H. J., Stähli, M. and Seibert, J.: Is groundwater response timing in a pre-alpine catchment controlled more by topography or by rainfall?, Hydrol. Process., 30(7), 1036–1051, doi:10.1002/hyp.10634, 2016.

Rinderer, M., McGlynn, B. L. and van Meerveld, H. J.: Groundwater similarity across a watershed derived from time-warped and flow-corrected time series, Water Resour. Res., 53(5), 3921–3940, doi:10.1002/2016WR019856, 2017.

Rodhe, A. and Seibert, J.: Groundwater dynamics in a till hillslope: Flow directions, gradients and delay, Hydrol. Process., 25(12), 1899–1909, doi:10.1002/hyp.7946, 2011.

Rosenbaum, U., Bogena, H. R., Herbst, M., Huisman, J. A., Peterson, T. J., Weuthen, A., Western, A. W. and Vereecken, H.: Seasonal and event dynamics of spatial soil moisture patterns at the small catchment scale, Water Resour. Res., 48(10), doi:10.1029/2011WR011518, 2012.

Saffarpour, S., Western, A. W., Adams, R. and McDonnell, J. J.: Multiple runoff processes and multiple thresholds control agricultural runoff generation, Hydrol. Earth Syst. Sci., 20(11), 4525–4545, doi:10.5194/hess-20-4525-2016, 2016.

Scheliga, B., Tetzlaff, D., Nuetzmann, G. and Soulsby, C.: Groundwater dynamics at the hillslope–riparian interface in a year with extreme winter rainfall, J. Hydrol., 564(May), 509–528, doi:10.1016/j.jhydrol.2018.06.082, 2018.

Silasari, R., Parajka, J., Ressl, C., Strauss, P. and Blöschl, G.: Potential of time-lapse photography for identifying saturation area dynamics on agricultural hillslopes, Hydrol. Process., 31(21), 3610–3627, doi:10.1002/hyp.11272, 2017.

Széles, B., Broer, M., Parajka, J., Hogan, P., Eder, A., Strauss, P. and Blöschl, G.: Separation of Scales in Transpiration Effects on Low Flows: A Spatial Analysis in the Hydrological Open Air Laboratory, Water Resour. Res., 54(9), 6168–6188, doi:10.1029/2017WR022037, 2018.

Therneau, T. and Atkinson, B.: rpart: Recursive Partitioning and Regression Trees. R package version 4.1-15, [online] Available from: https://cran.r-project.org/package=rpart%0A, 2019.

Tromp-van Meerveld, H. J. and McDonnell, J. J.: Threshold relations in subsurface stormflow: 2. The fill and spill hypothesis, Water Resour. Res., 42(2), doi:10.1029/2004WR003800, 2006.

Vidon, P. G. F. and Hill, A. R.: Landscape controls on the hydrology of stream riparian zones, J. Hydrol., 292(1–4), 210–228, doi:10.1016/J.JHYDROL.2004.01.005, 2004.

Weiss, A.: Topographic position and landforms analysis - Poster Conference, ESRI User Conf. San Diego, CA, 64, 227–245, doi:http://www.jennessent.com/downloads/TPI-poster-TNC_18x22.pdf, 2001.

Western, A. W., Blöschl, G. and Grayson, R. B.: Toward capturing hydrologically significant connectivity in spatial patterns, Water Resour. Res., 37(1), 83–97, doi:10.1029/2000WR900241, 2001.

Zhang, B., Tang, J. L., Gao, C. and Zepp, H.: Subsurface lateral flow from hillslope and its contribution to nitrate loading in streams through an agricultural catchment during subtropical rainstorm events, Hydrol. Earth Syst. Sci., 15(10), 3153–3170, doi:10.5194/hess-15-3153-2011, 2011.

Zuecco, G., Penna, D., Borga, M. and van Meerveld, H. J.: A versatile index to characterize hysteresis between hydrological variables at the runoff event timescale, Hydrol. Process., 30(9), 1449–1466, doi:10.1002/hyp.10681, 2016.